

# FYSRE Work Term Report

Kenji Kojima Group, CMMS

Cyrus Young, September 2022

## Table of Contents:

<b>Introduction:</b>	<b>4</b>
How to produce muons:	4
Detection Process:	5
<b>Simulation and Analysis:</b>	<b>5</b>
Analysis of Simulation Results:	11
Simulation limitations:	14
Important MATLAB Tools:	14
<b>Linear Interpolation:</b>	<b>15</b>
Linear Interpolation (No Magnetic Field):	15
x position vs number of positrons (Downstream, no magnetic field):	16
y position vs number of positrons (Downstream, no magnetic field):	16
x position vs number of positrons (Upstream, no magnetic field):	18
x position vs number of positrons (Upstream, no magnetic field):	18
Linear Interpolation ( $B = 0.1 \text{ T}$ ):	19
x position vs number of positrons (Downstream, $B = 0.1 \text{ T}$ ):	19
y position vs number of positrons (Downstream, $B = 0.1 \text{ T}$ ):	19
Summary of x-position Distribution for the Upstream Detectors:	20
Important Note:	20
Summary of x-position Distribution for the Downstream Detectors:	21
Exit Tangent:	21
Adding a Cryostat wall:	22
<b>Quadratic Interpolation:</b>	<b>24</b>
Comparison of Two Detectors vs Three Detectors in a $0.2 \text{ T}$ magnetic field:	24
Increasing the field to $0.3 \text{ T}$ with Three Detectors:	27

Increasing the field to 0.4 T with Three Detectors:	29
Increasing the field to 0.5 T with Three Detectors:	30
<b>Helical Approximation with Front Detectors:</b>	<b>30</b>
Helical Approximation for $B = 0.1 \text{ T}$ vs $B = 0.3 \text{ T}$ :	32
Helical Approximation for $B=0.3 \text{ T}$ vs $B=0.5 \text{ T}$ :	33
Helical Approximation for $B=0.01 \text{ T}$ vs $B=0.1 \text{ T}$ :	33
Helical Approximation for $B=0.001 \text{ T}$ vs $B=0.01 \text{ T}$ :	34
Helical Approximation for $B=0.3 \text{ T}$ vs $B=3 \text{ T}$ :	35
Helical Approximation Result Analysis	36
Comparing Standard Deviation of data with magnetic field strength:	36
Comparing Efficiency (Counts in the 4 central bins / number of positrons detected) of data with magnetic field strength:	37
Helical Approximation Comparison, Steel Cryostat vs No Cryostat:	38
Helical Approximation, Aluminum Cryostat vs Stainless Steel Cryostat for $B = 0.3 \text{ T}$ :	39
Helical Approximation, Real detectors vs Cryostat:	40
Helical Approximation with target offset from the center:	41
Graph of Standard Deviation vs Rounding number:	41
Helical Approximation but Scaled Down by 5:	43
Symmetric Detector Placement vs Asymmetric Detector Placement for Scaled Down Scenario:	44
Helical Approximation but scaled down by 25:	45
Helical Approximation but scaled down by 2 and 4:	46
Helical Approximation but scaled down by 10:	47
Helical Approximation but with approximation value shifted to $z = -0.3$ :	48
<b>Helical Approximation with Bottom Detectors</b>	<b>49</b>
Helical Approximation with Bottom Detectors vs Front Detectors for $B = 0.3 \text{ T}$ :	50
Momentum Distribution for Bottom Detector Set-up (High Level Approximation):	51
Standard Deviation vs Rounding Number:	53
Helical Approximation with Bottom Detectors but scaled down:	54
<b>Helical Approximation with Solenoids:</b>	<b>55</b>
Front-Back Setup (Large Current):	55
Front-Back Setup (Small Current):	57
Up-Down Setup:	59
<b>Helical Approximation with Ideal Helmholtz Coil:</b>	<b>60</b>
Front-Back Setup:	60
Front-Back Setup (10x Less Current as before):	61
Up-Down Setup:	62

<b>LAMPF Spectrometer Helmholtz Simulation:</b>	<b>63</b>
Front-Back Setup:	63
Up-Down Setup:	64
<b>Conclusion:</b>	<b>65</b>
<b>Appendix 1: Conference Poster</b>	<b>66</b>

## Introduction:

Due to their strong magnetic moment, muons are extensively used as a magnetometer in materials science, used to study superconductors, semiconductors, and magnetism. A common use of muons is to implant them within a material of study with a 100% spin polarization (this way, the muons all follow the same path and thus can be used to study the magnetic field of the material in more detail).

For this experiment, we will be taking advantage of muon decay. A beam of positive muons ( $\mu^+$ ) is fired at a target (usually aluminum, carbon, or silver). The muons are stopped by the target, and the muons will eventually decay into a positron (which is usually emitted along the muon spin), an electron neutrino and a muon antineutrino as shown below:

$$\mu^+ \rightarrow e^+ + \nu_e + \bar{\nu}_\mu$$

The emitted positrons will be detected by pairs of detectors on each side. Studying the paths the positrons make will help us learn more about the properties of muons. Note: since neutrinos are much harder to detect than positrons, they are effectively ignored in the experiment.

## How to produce muons:

A proton beam is fired in a target, usually made of beryllium. The following equation describes the interaction that takes place between the protons that are fired at a target and the protons within the target itself:

$$p + p \rightarrow \pi^+ + p + n$$

The pion ( $\pi^+$ ) will decay into a muon neutrino and a positive muon. Note that the total spin and momentum is conserved after the decay.

$$\pi^+ \rightarrow \mu^+ + \nu_\mu$$

The muons are then controlled by magnetic fields and directed as a beam.

## Detection Process:

In order to gain necessary data needed for muon analysis, we need to have a pair of detectors together lined up in front of each other in all directions; front-back, left-right, top-bottom (see Figure 1 for a visual). This way, we can easily work out the path the positron made through the detectors by extrapolating the path made by the points that the positron made with the detectors when they struck the detector. The detectors themselves are scintillation detectors which are able to convert high energy radiation such as X or gamma-rays to a near visible or visible light (<https://web.stanford.edu/group/scintillators/scintillators.html#:~:text=Scintillators%20are%20materials%20that%20are,Knoll>).

## Simulation and Analysis:

We first need to download G4beamline to run our simulations. G4beamline is a user-friendly yet comprehensive tool for particle physics simulations. To download G4beamline, go to <http://www.muonsinternal.com/muons3/G4beamline> and download the version which matches your OS.

The GUI of G4beamline will give a set of instructions to follow in order to run the simulations. In order to run the simulation, we have to write an input file which outlines parameters such as particles used, location and number of detectors and then select that input file to be used for a simulation.

A comprehensive user guide is shown below:

<https://beamdocs.fnal.gov/AD/DocDB/0079/007950/001/G4beamlineUsersGuide.pdf>

The guide outlines the basic concepts, the possible commands, and also gives several coded examples of possible scenarios to simulate. If we run the simulations without the visualizer on, an output file (or multiple output files, depending on the situation) is generated in Ntuple format. We can then use a data analysis tool (such as MATLAB) to analyze and visualize the data. To do so, we use the following command below in MATLAB:

```
[x1 y1 z1 Px1 Py1 Pz1 t1 PDGid1 EventID1 TrackID1 ParentID1 Weight1]
= ...
textread('<input file>',...
'%n %n %n %n %n %n %n %n %n %n',...
```

```
'commentstyle', 'shell') ;
```

Where <input file> is the file you want to read the data off of. In our case, the file is in the form:

`filename.txt`

Where filename is usually the name of a specific detector (like Detector1.txt). We obtain one input file per detector which contains the following information below (from page 22 of the user guide):

Name	Description
x, y, z.	The position of the track, in the selected coordinates. Millimeters.
Px, Py, Pz	The momentum of the track, in the selected coordinates. MeV/c.
t	The global time of the track. Nanoseconds
PDGid	The ID of the particle, using the assigned value from the Particle Data Group.
EventID	The event number.
TrackID	The track identifier.
ParentID	The track identifier for this track's parent; 0 if this is a beam track.
Weight	Weight The weight of the track (defaults to 1.0)

Using a significantly altered version of the “MultipleScattering.g4bl” file in the guide, we can create the following simulation below. The purple squares are detectors and the gray circle is a carbon target. The Blue lines are muon beams and the red lines are positron beams which, along with electron and muon neutrinos (not shown in Figure 1), are the results of muon decay. The code for the input file is below:

```
*      Good Copy file
#
```

```

#      Multiple scattering and ionization energy loss in materials.
#
#      lengths are mm; momentum is MeV/c, density is gm/cm^3
#
#      Magnetic Field strength in Teslas (T)

physics QGSP_BIC_EMZ
setdecay mu+ lifetime=2197 e+,nu_e,anti_nu_mu=1.0

beam gaussian polarization=0,0,-1 particle=mu+ meanMomentum=30
nEvents=10000 z=-1250 sigmaX=2 sigmaY=2

fieldexpr F height=600 width=600 length=1000 Bz=1
place F z=-250

fieldlines exit=1 center=0,0,-250 nLines=100

particlecolor mu+=0,0,1 e+=1,0,0, nu_e=0.3,0.3,0.3,
anti_nu_mu=0.5,0,0.5

trackcuts keep=mu+,e+,nu_e,anti_nu_mu kineticEnergyCut=0

material C A=12.011 Z=6 density=2
tubs Target1 outerRadius=50 material=C length=1 color=0.7,0.7,0.7

detector Det width=60 height=60 length=5 color=1,0,1
require='PDGid==11'
detector BackDet radius=30 innerRadius=5 length=5 color=1,0,1
require='PDGid==11'

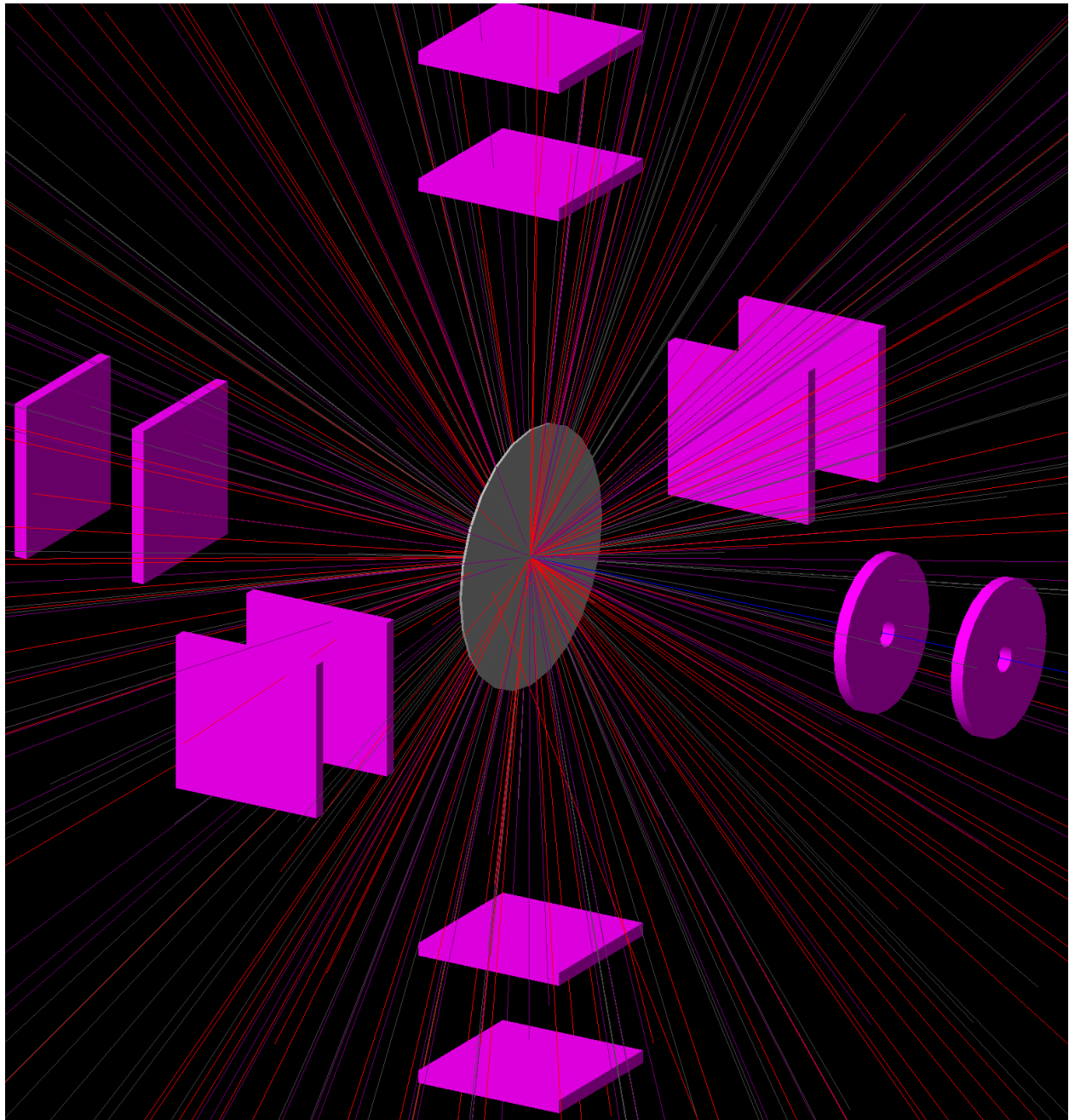
place Target1 z=0

place Det x=100 z=0 rotation=Y90 rename=LeftSideDetector
place Det x=-100 z=0 rotation=Y90 rename=RightSideDetector
place Det y=100 z=0 rotation=X90 rename=CloseTopDetector
place Det y=-100 z=0 rotation=X90 rename=CloseBottomDetector
place Det z=100 rename=CloseFrontDetector
place BackDet z=-100 rename=CloseBackDetector

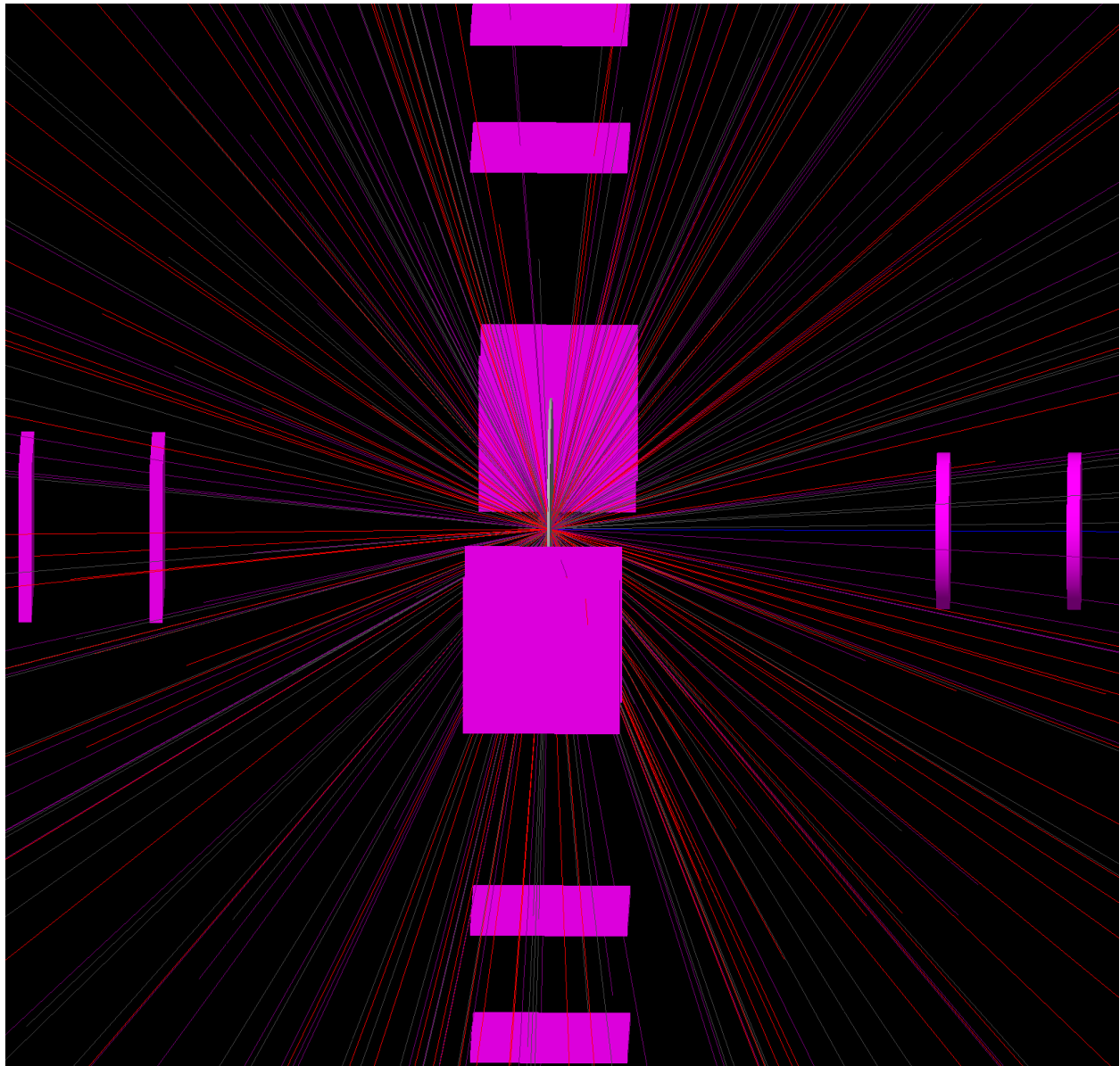
place Det x=150 z=0 rotation=Y90 rename=FarLSDetector
place Det x=-150 z=0 rotation=Y90 rename=FarRSDetector
place Det y=150 z=0 rotation=X90 rename=FarTopDetector
place Det y=-150 z=0 rotation=X90 rename=FarBottomDetector
place Det z=150 rename=FarFrontDetector
place BackDet z=-150 rename=FarBackDetector

```

From the code, we can see that the appropriate detectors as well as the carbon target were all placed. We further improved the simulation via the require='PDGid==11' command which ensures that the detectors only detect positrons, which is consistent with our physical detectors. The incorporated physics package, QGSP\_BIC\_EMZ, allows for more accurate simulations at lower energies (we could have alternatively used QGSP\_BERT, which is also built for simulations at lower energy levels) and more accurate simulations in regards to positron dynamics. We also have successively incorporated a 100% spin polarized muon beam in which the beam's constituent muons decay into positrons with a correct muon lifetime of 2197 ns. Lastly, using the “fieldexpr” command, we have successfully inporated a 1 Tesla magnetic field in the z-direction. Although the dimensions and placement of the detectors themselves are not correct, they are very easy to fix.



Diagonal front view (Figure 1)



Side view (Figure 2)

## Analysis of Simulation Results:

An altered version of the original file is used in order to get rid of extraneous detectors and data that were not relevant to the simulation. Below is the code for the altered input file:

```

physics QGSP_BIC_EMZ
setdecay mu+ lifetime=2197 e+,nu_e,anti_nu_mu=1.0

beam gaussian polarization=0,0,-1 particle=mu+ meanMomentum=30
nEvents=10000 z=-1000
particlecolor mu+=0,0,1 e+=1,0,0, nu_e=0.3,0.3,0.3,
anti_nu_mu=0.5,0,0.5
trackcuts keep=mu+,e+,nu_e,anti_nu_mu kineticEnergyCut=0

material C A=12.011 Z=6 density=2
tubs Target1 outerRadius=50 material=C length=1 color=0.7,0.7,0.7

virtualdetector VirtDet radius=50 innerRadius=1 length=5 color=1,0,1
require='PDGid==11'

place Target1 z=250

place VirtDet z=200 rename=VirtBackDet
place VirtDet z=300 rename=VirtFrontDet

```

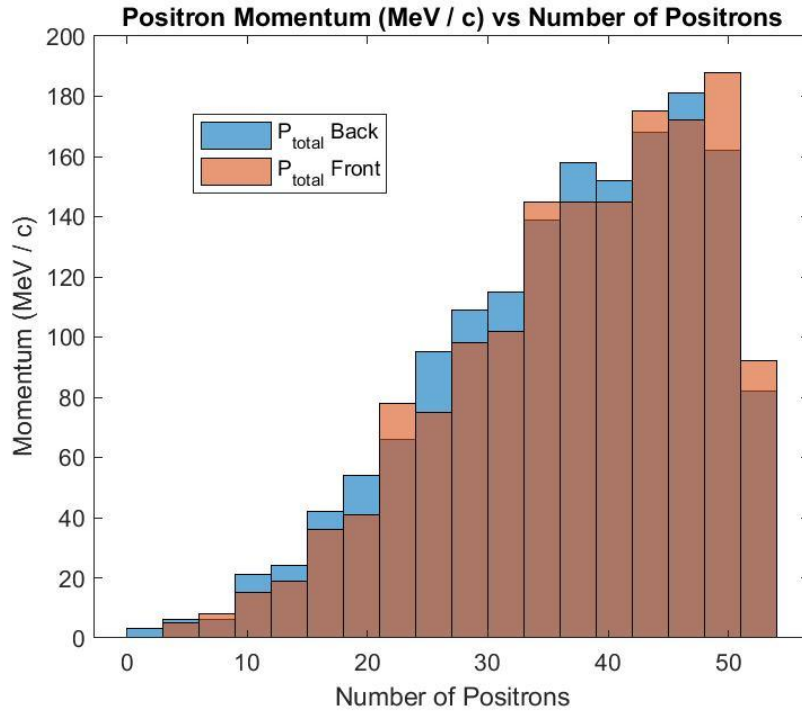
In order to gain the relevant information we need to learn more about muons, we need to analyze the momentum distributions of the positrons that resulted as a decay product of the muons. The tuple files that g4beamline produces contains the values of the momentum of the positrons detected by each detector in the  $x$ ,  $y$ , and  $z$  directions for each separate positron. Therefore, all we need to find is:

$$P = \sqrt{P_x^2 + P_y^2 + P_z^2}$$

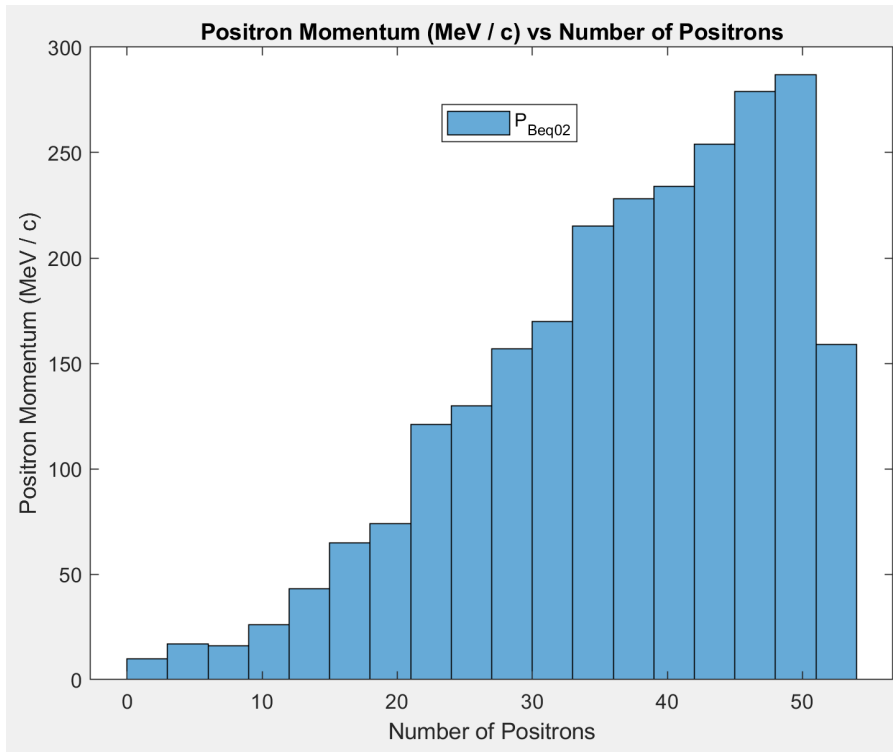
for each separate positron and then graph the results. Here columns A, B, and C are  $P_x$ ,  $P_y$ , and  $P_z$  respectively and column D is the total magnitude of momentum, all in MeV / c for the front detector. We carry out a very similar procedure for the back detector as well.

	A	B	C	D	E	F
1	6.57007	-7.23973	20.294	22.52612	<- Front Det	
2	-0.29279	11.6874	34.1933	36.13672		
3	19.8053	9.98309	23.4975	32.31168		
4	-4.95269	22.2088	29.1498	36.97933		
5	8.01153	18.5337	44.2189	48.61063		
6	-5.31068	10.6062	33.8496	35.86768		
7	-31.6579	18.068	37.8162	52.52371		
8	-22.856	12.9922	37.435	45.74465		
9	-3.80059	19.1192	28.4023	34.44821		
10	14.0303	-28.6974	38.9894	50.404		
11	-24.8453	-8.24389	35.5183	44.12256		
12	32.8481	-2.60032	39.6285	51.53812		
13	-3.84981	15.5361	16.1278	22.72218		
14	-0.02906	-7.05448	21.6346	22.75571		
15	1.14587	-22.8424	24.8644	33.78353		
16	13.0197	-22.2201	38.2375	46.10154		
17	-27.5854	-8.57454	27.7745	40.07368		
18	17.4375	2.11632	39.4848	43.21568		
19	-3.9874	21.789	26.005	34.16021		
20	-1.3852	16.9164	35.7191	39.54665		
21	7.97916	4.66639	40.9561	41.98624		
22	-2.00063	10.8375	32.6944	34.50185		
23	-24.4273	-3.13867	32.2937	40.61314		
24	-15.448	-15.0793	22.5943	31.24945		
25	-10.5047	3.75928	28.8134	30.89811		
26	8.34042	-3.30688	28.4829	29.86258		
27	-2.80084	-0.75612	11.4153	11.77818		
28	-9.88432	-1.59148	37.935	39.23387		

Once we have calculated the total magnitude of momentum for each positron for both detectors, we can graph the results. Using a histogram, we get:



The shape of the graph above (with no magnetic field) agrees with experimental results. Now we will run a similar simulation but with a 0.2 T magnetic field. Below is the momentum distribution for positrons inside the magnetic field.



## Simulation limitations:

Since g4beamline was designed for high energy beams (Gev to Tev), there was some concern regarding the accuracy of the simulation for lower energy beams (such as the kev to Mev) range. We mitigated some of the potential inaccuracy that would be present in lower energy simulations by incorporating the QGSP\_BIC physics package (QGSP\_BERT could have equivalently been used, but both gave very similar results). After some research on the g4beamline forum, I read that the “physics QGSP\_BIC\_EMZ” package is good for simulating the scattering of positrons and electrons below energies of 100 Mev. Below is a comparison of two simulations, one in which I invoke the QGSP\_BIC\_EMZ package and the other in which the QGSP\_BERT package is used instead (with spinTracking on).

## Important MATLAB Tools:

Fitting data to a curve (particularly a gaussian curve) is crucial to successfully analyze data with scrutiny. A method to do this in MATLAB is to divide the data into N numbers of equally spaced bins and then to use the Curve Fitting app.

Knowing how to plot histograms is also crucial to success in MATLAB

## Linear Interpolation:

### Linear Interpolation (No Magnetic Field):

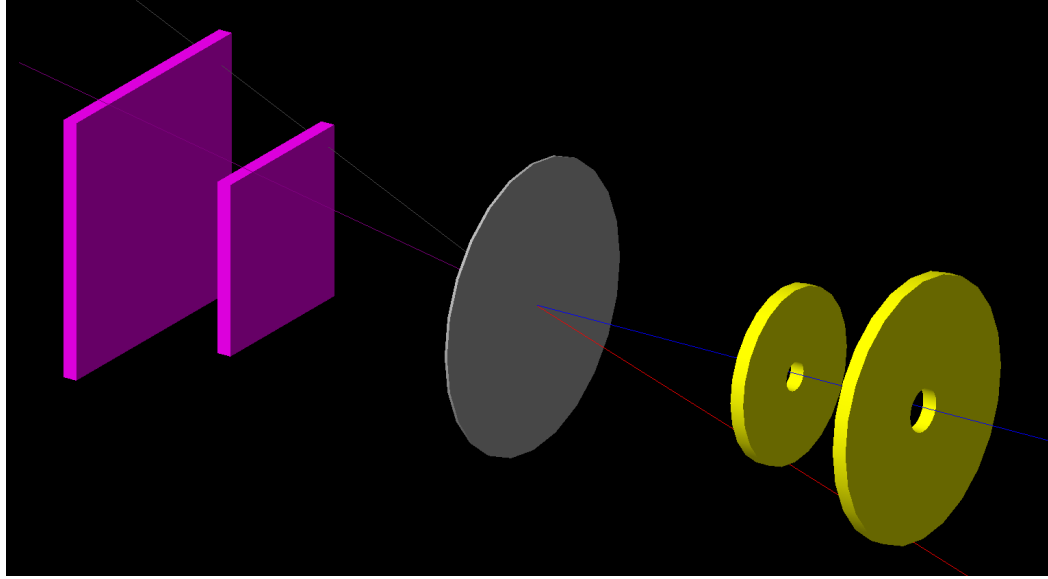
In this section, we analyzed the origin of the positrons using the linear interpolation algorithm (see formula below). Like before, we fired a muon beam at a target. The beam then decayed into positrons which then traveled through two virtual detectors (virtual detectors detect the particles and some of their properties, such as momentum and the time it hits the detector, but do not affect their trajectories). We then tracked the points that the positron beam made with the two detectors and used linear interpolation to find the  $x$  and  $y$  coordinates the beam made with the target. The horizontal axis represents the number of positrons and the vertical axis represents the distance from the center of the target (in the  $x$  and  $y$  directions) in mm.

The linear interpolation formula is shown below. Here,  $(x_1, y_1)$  and  $(x_2, y_2)$  are the two known sets of points.

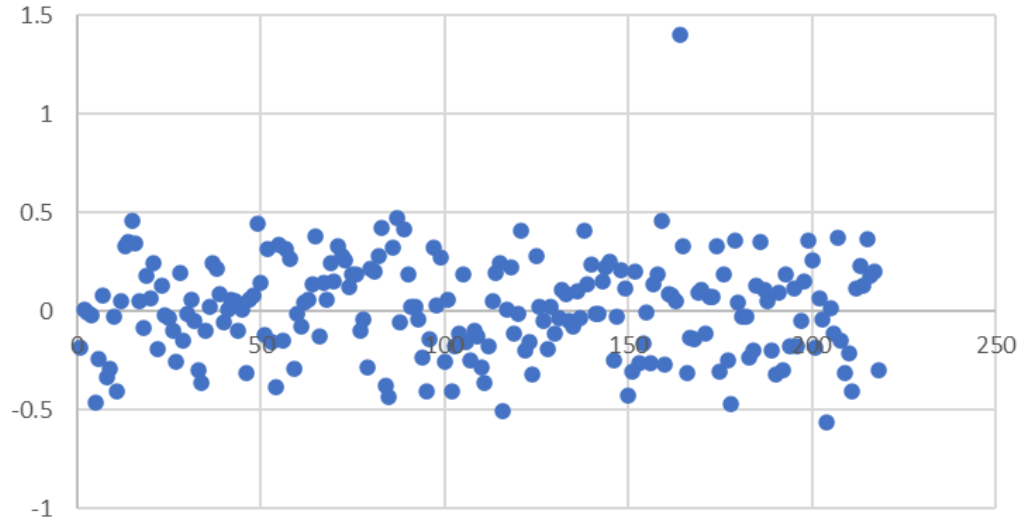
$$y - y_1 = \frac{y_2 - y_1}{x_2 - x_1} (x - x_1)$$

(Note: “Downstream” refers to all positrons which are detected in the direction of the beam and passed through the target, while “Upstream” refers to all positrons which are detected opposite to the direction of the beam, namely the ones which were reflected off of the target.)

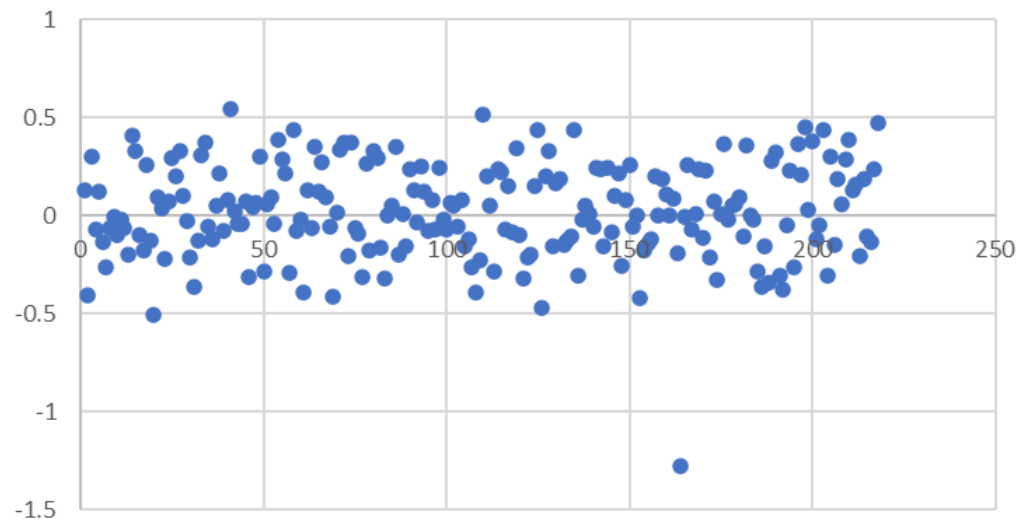
The simulation of the setup is shown below. The pink square-shaped detectors are the so-called “Front Detectors” (or Upstream detectors) and the yellow circle detectors are the so-called “Back Detectors” (or Downstream detectors).



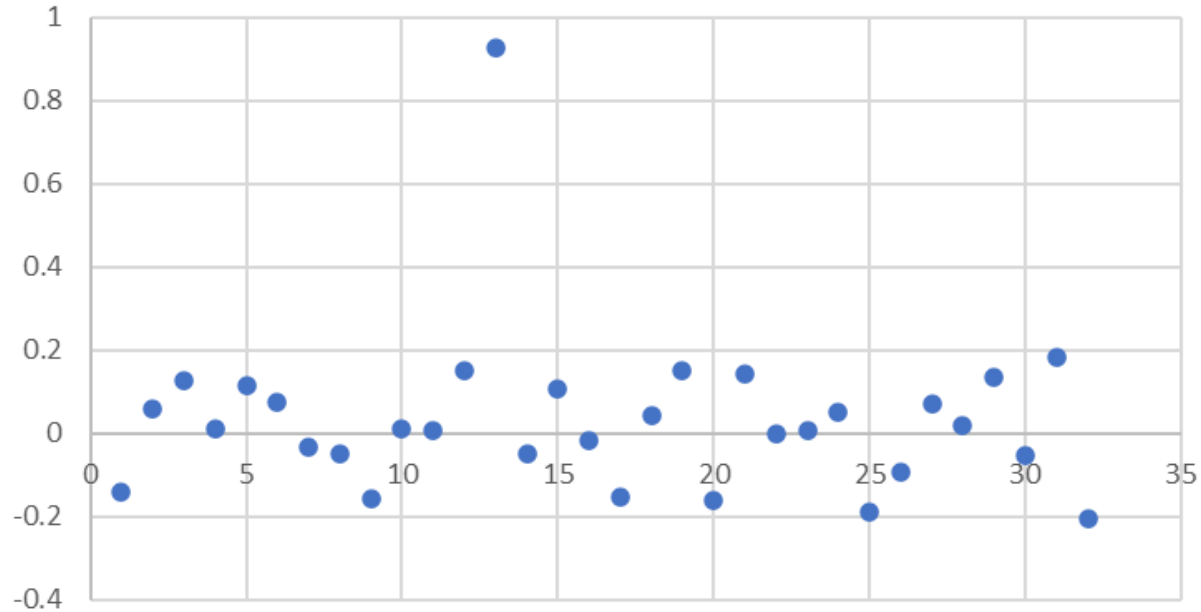
$x$  position vs number of positrons (Downstream, no magnetic field):



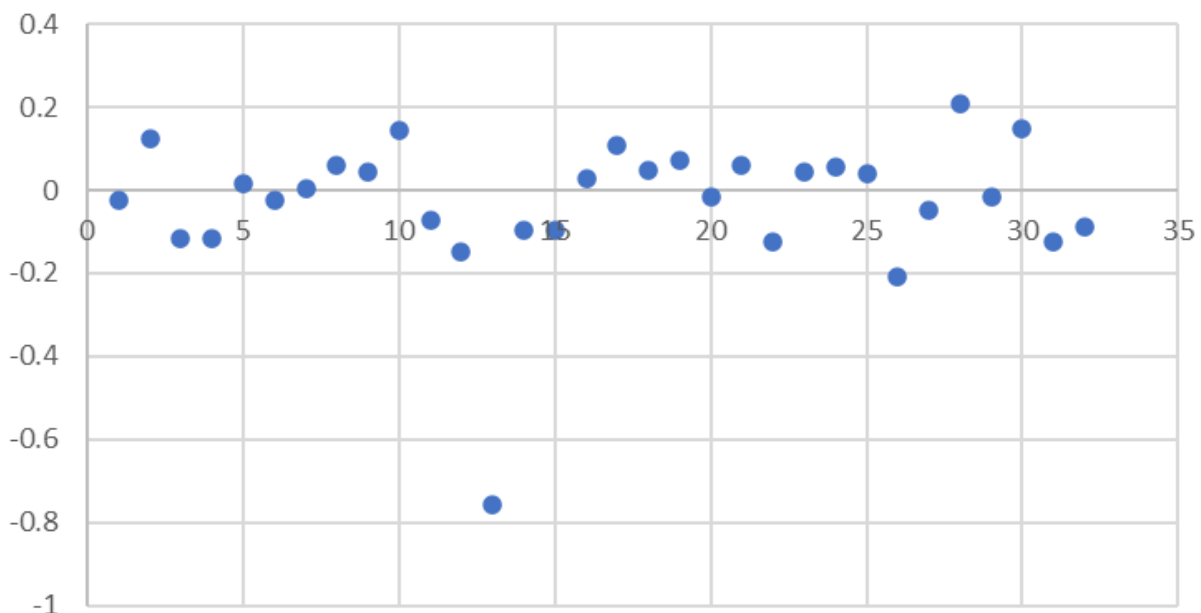
$y$  position vs number of positrons (Downstream, no magnetic field):



$x$  position vs number of positrons (Upstream, no magnetic field):

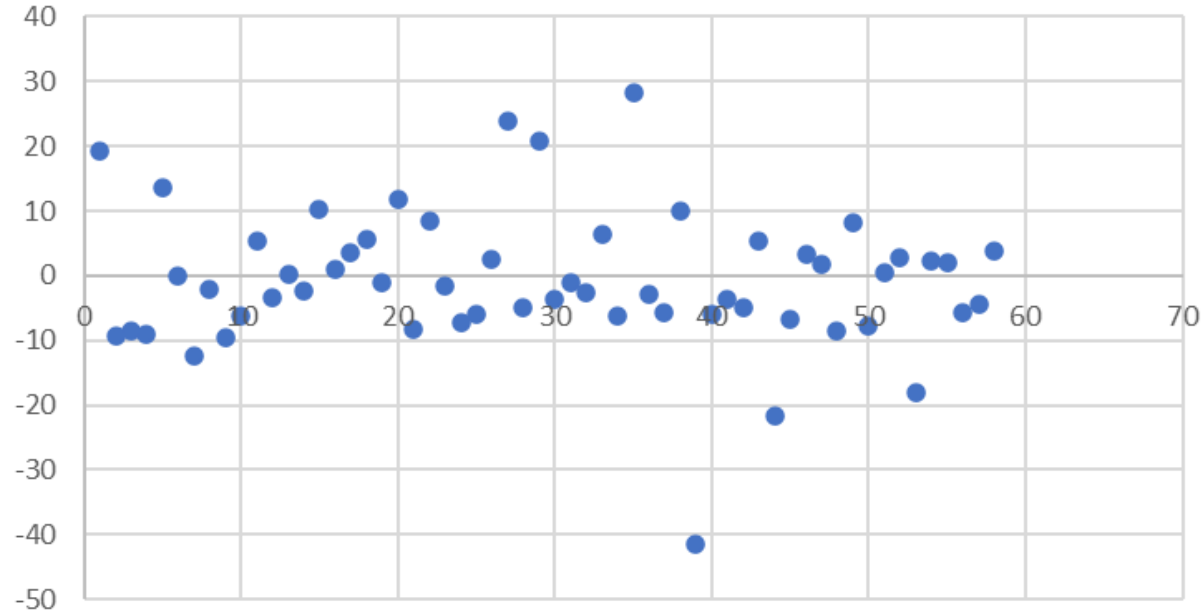


$x$  position vs number of positrons (Upstream, no magnetic field):

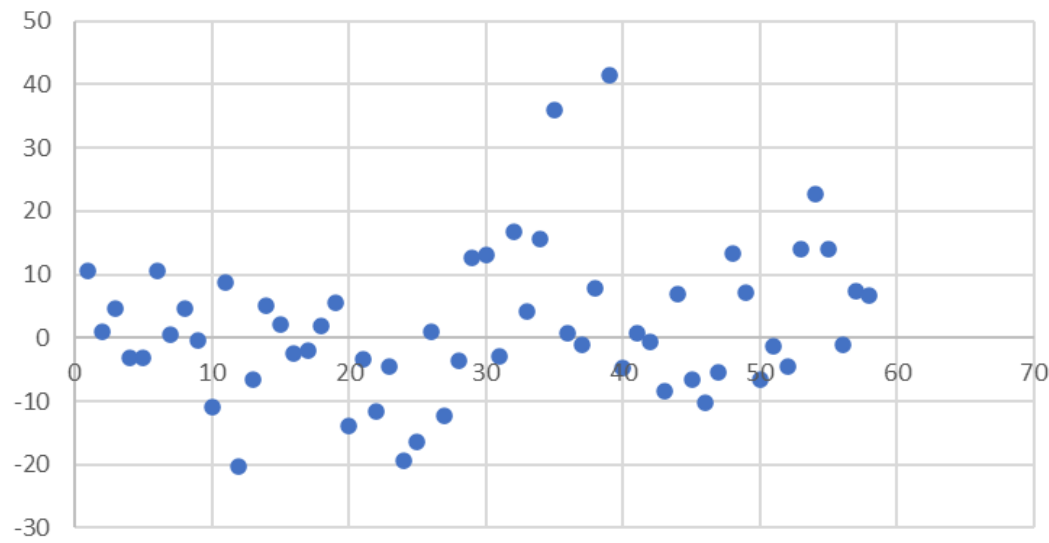


Linear Interpolation ( $B = 0.1$  T):

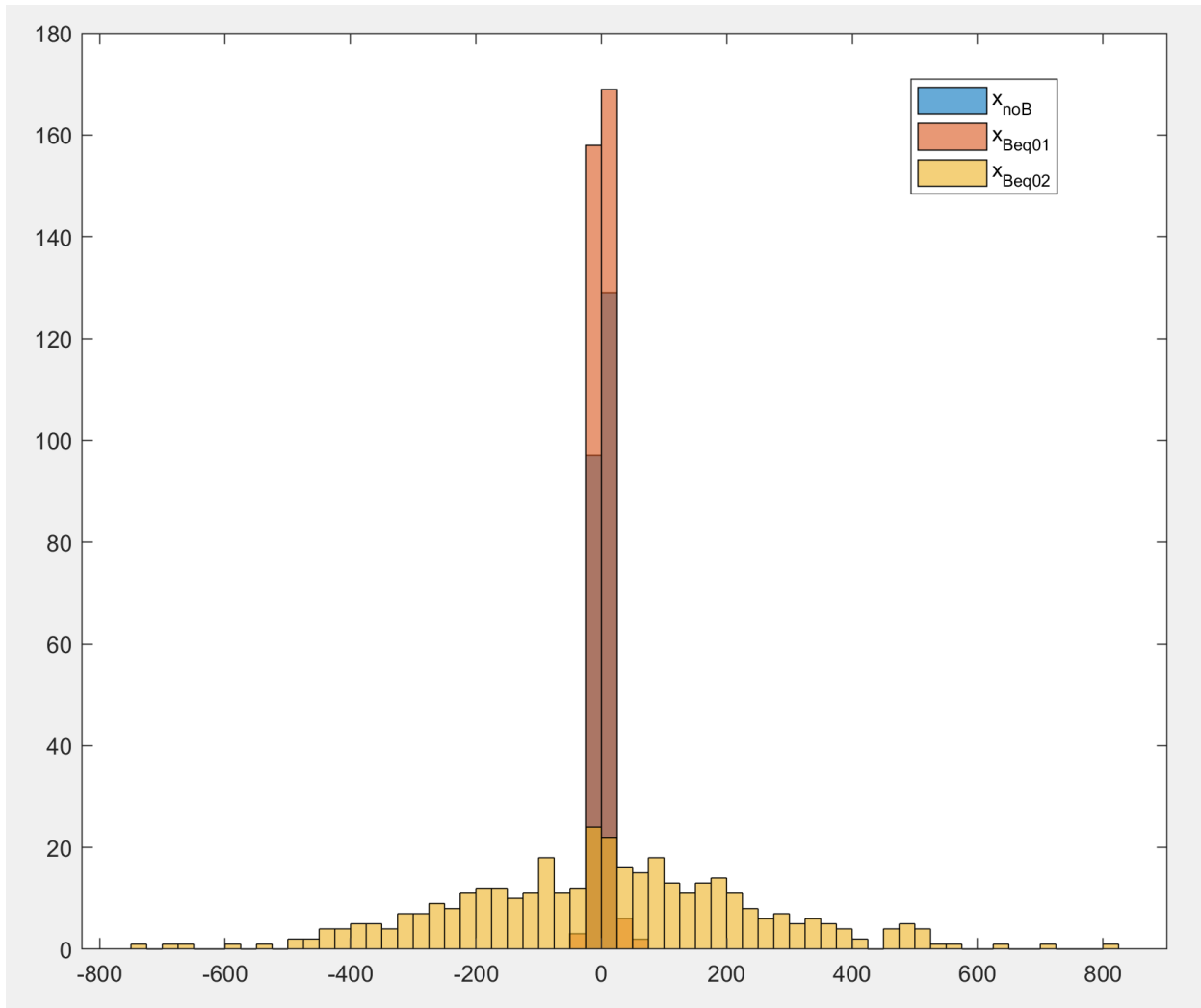
$x$  position vs number of positrons (Downstream,  $B = 0.1$  T):



$y$  position vs number of positrons (Downstream,  $B = 0.1$  T):



## Summary of $x$ -position Distribution for the Upstream Detectors:

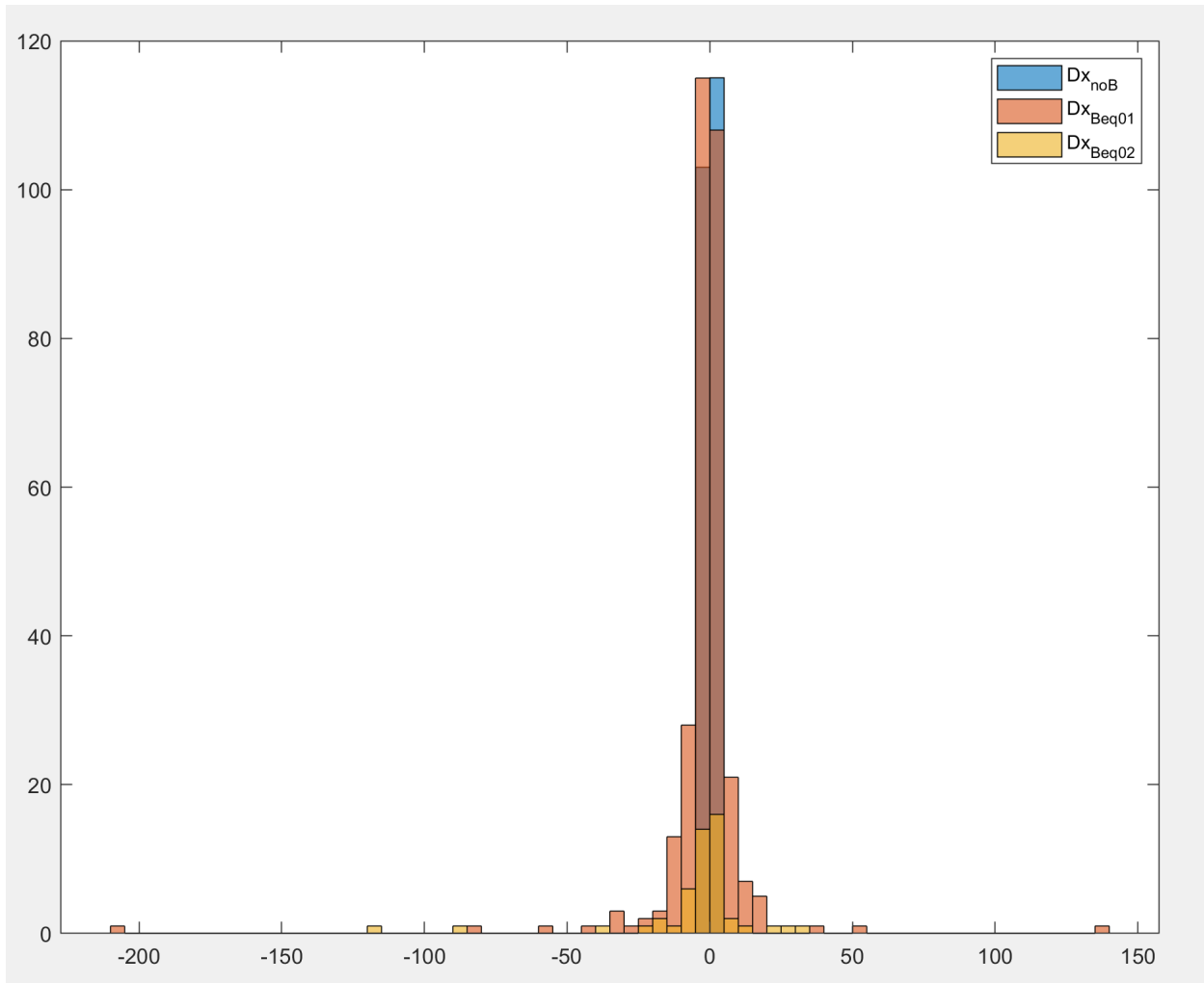


Due to the increased curvature that results due to higher magnetic fields, there was a dramatic increase in positron distribution as we changed the field from 0.1 T to 0.2 T.

### Important Note:

Positrons in the  $B=0.1$  T field were more evenly distributed than the positrons with no field. The only reason why there are more positrons at  $x = 0$  with  $B = 0.1$  T is because there were more positrons generated in total.

## Summary of $x$ -position Distribution for the Downstream Detectors:



Consistent with the results of the upstream detectors, the linear approximation algorithm diminished in accuracy for stronger magnetic fields.

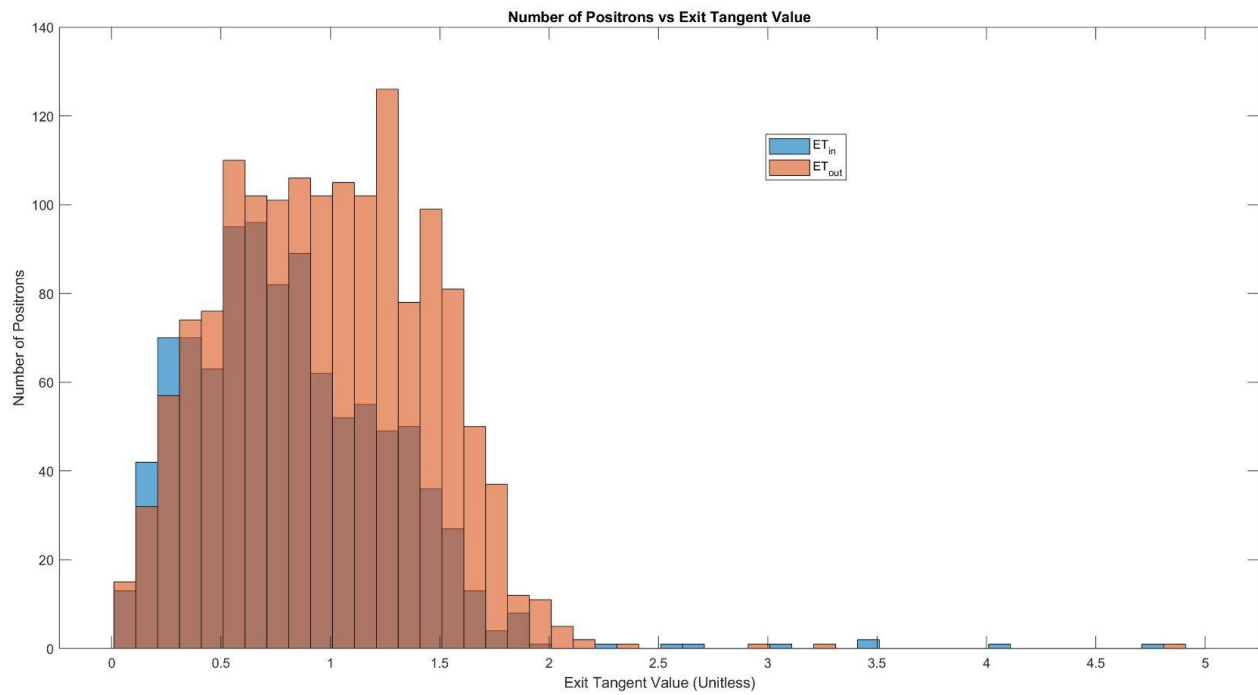
## Exit Tangent:

The Exit Tangent is defined as:

$$E_{tan} = \frac{\sqrt{P_x^2 + P_y^2}}{P_z}$$

Note that particles whose trajectory is aimed mostly in the z-direction (central particles) are more likely to have lower  $E_{tan}$  value as most of its momentum is in the z-direction. Conversely,

Particles which scatter away from the central region are more likely to have a higher value of  $E_{tan}$  (as they have more momentum in the  $x$  and  $y$ , and  $z$  directions but lower momentum in the  $z$  direction. This analysis is confirmed by the figure below. The graph portrays the number of positrons vs Exit Tangent value for all the particles in one of our simulations.  $ET_{in}$  is the Exit Tangent value for particles near the center, while  $ET_{out}$  is the Exit Tangent value for particles located in the outer edges.



### Adding a Cryostat wall:

If we add a solid wall in front of the detector, low energy positrons will be blocked out and positrons with an initial higher energy will lose some energy due to impact with the cryostat. This is supported by the graph below which shows that many more high-momentum (and thus high-energy) positrons are detected if a cryostat is removed. The code for the simulation is shown below as well. The simulation uses a uniform 0.2 T magnetic field in the z-direction.

```
*      Cryostat File
#
#      Multiple scattering and ionization energy loss in materials.
#
#      lengths are mm; momentum is MeV/c, density is gm/cm^3
```

```
physics QGSP_BIC_EMZ
setdecay mu+ lifetime=2197 e+,nu_e,anti_nu_mu=1.0

beam gaussian polarization=0,0,-1 particle=mu+ meanMomentum=30
nEvents=10000 z=-1250

fieldexpr F height=1000 width=1000 length=1000 Bz=0.2
place F z=-250

fieldlines exit=1 center=0,0,-250 nLines=100

particlecolor mu+=0,0,1 e+=1,0,0, nu_e=0.3,0.3,0.3,
anti_nu_mu=0.5,0,0.5

trackcuts keep=mu+,e+,nu_e,anti_nu_mu kineticEnergyCut=0

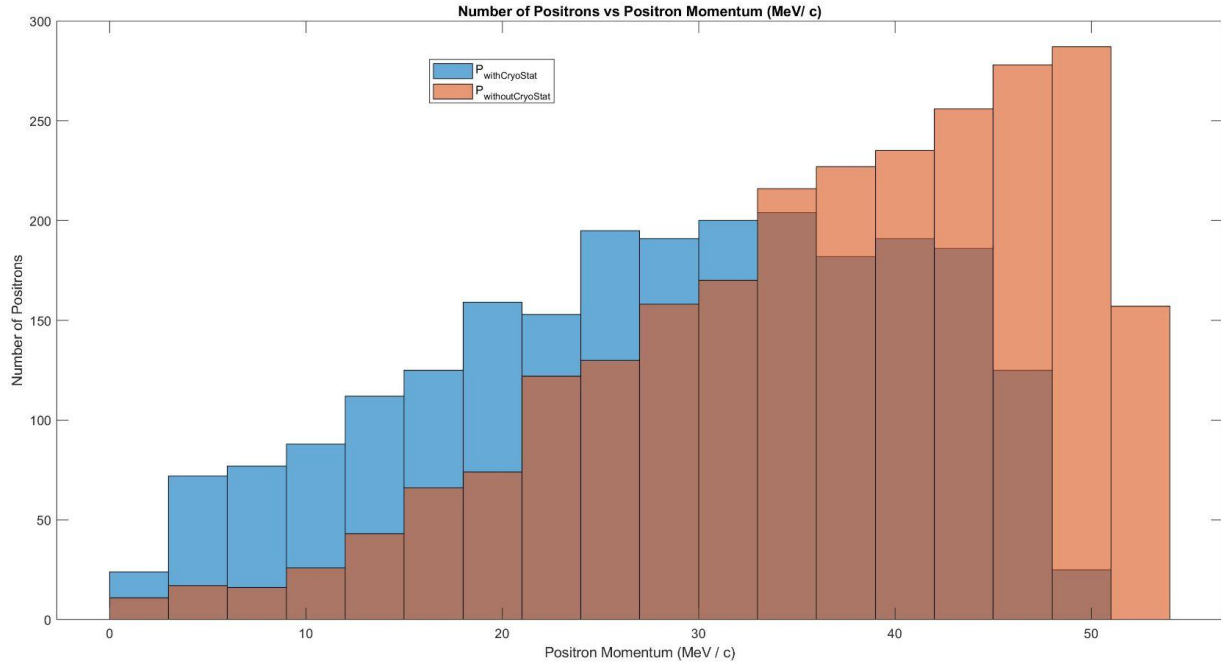
material C A=12.011 Z=6 density=2
tubs Target1 outerRadius=50 material=C length=1 color=0.7,0.7,0.7

virtualdetector Detclose width=300 height=300 length=5 color=1,0,1
require='PDGid==11'

place Target1 z=0

place Detclose z=100 rename=CloseFrontDetector
```

The blue bars represent the positrons detected with the cryostat present and the red bars represent the positrons detected without the cryostat.



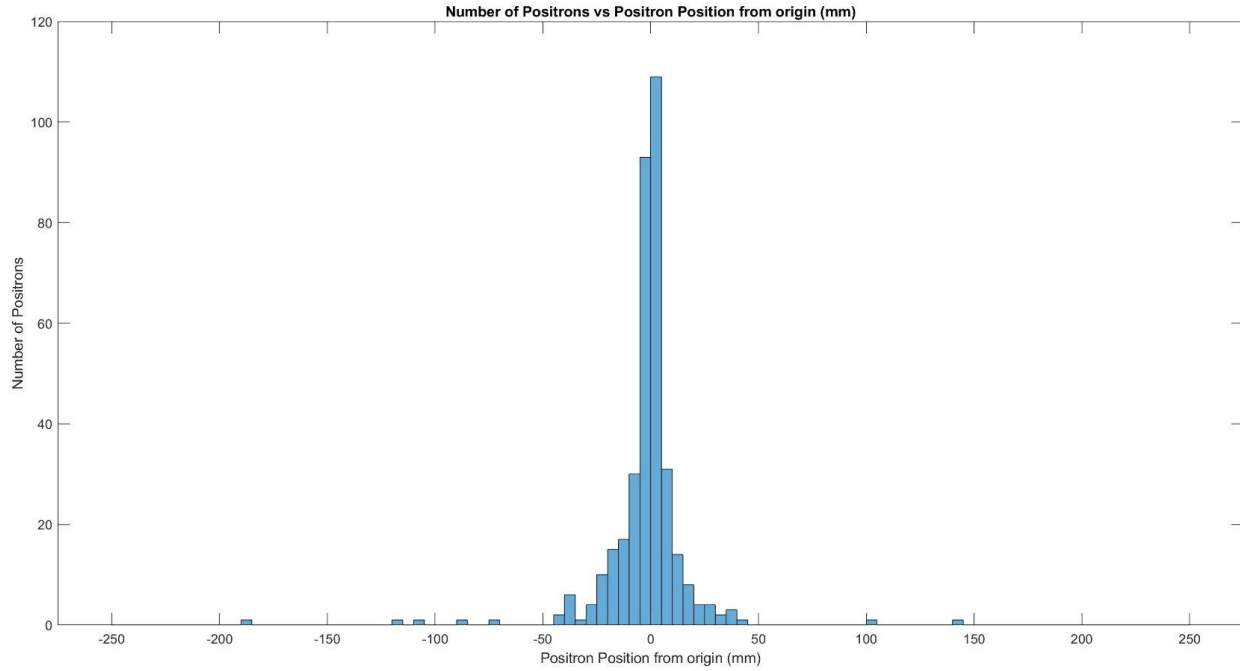
## Quadratic Interpolation:

In this section, we deal with detecting the positrons (with the exact same setup in the last section) using a quadratic interpolation algorithm. The quadratic interpolation algorithm can be described as follows. Take three points  $(x_1, y_1)$ ,  $(x_2, y_2)$  and  $(x_3, y_3)$  and use the formula below to find the formula of the curve.

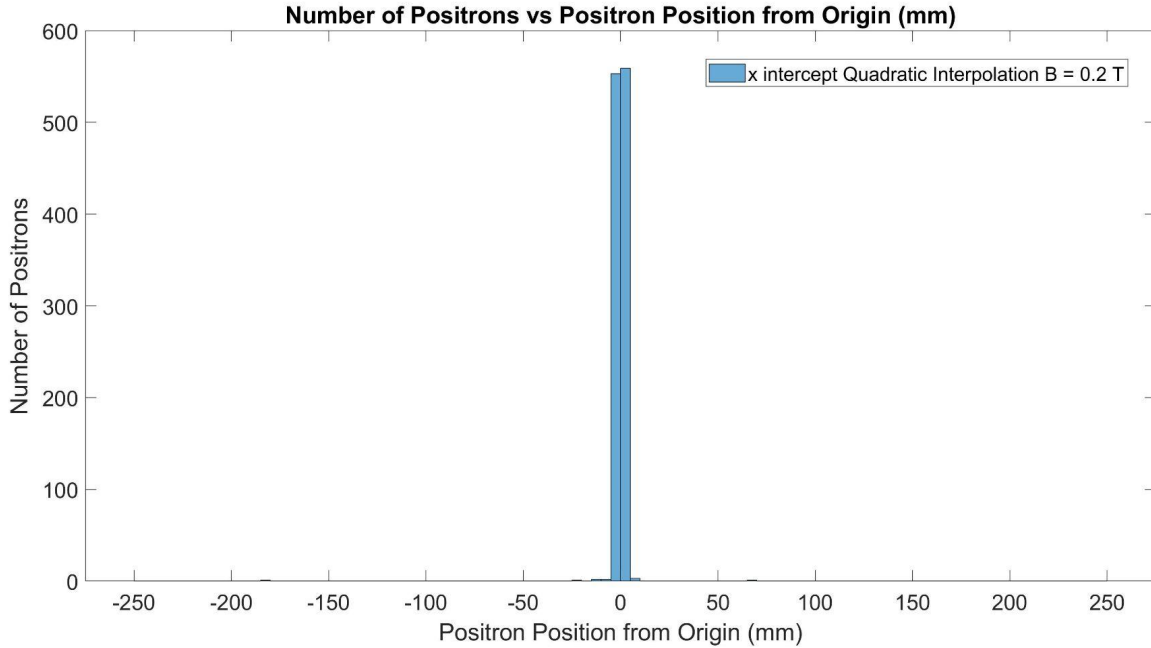
$$y = \frac{(x-x_1)(x-x_2)}{(x_0-x_1)(x_0-x_2)}y_0 + \frac{(x-x_0)(x-x_2)}{(x_1-x_0)(x_1-x_2)}y_1 + \frac{(x-x_0)(x-x_1)}{(x_2-x_0)(x_2-x_1)}y_2$$

## Comparison of Two Detectors vs Three Detectors in a 0.2 T magnetic field:

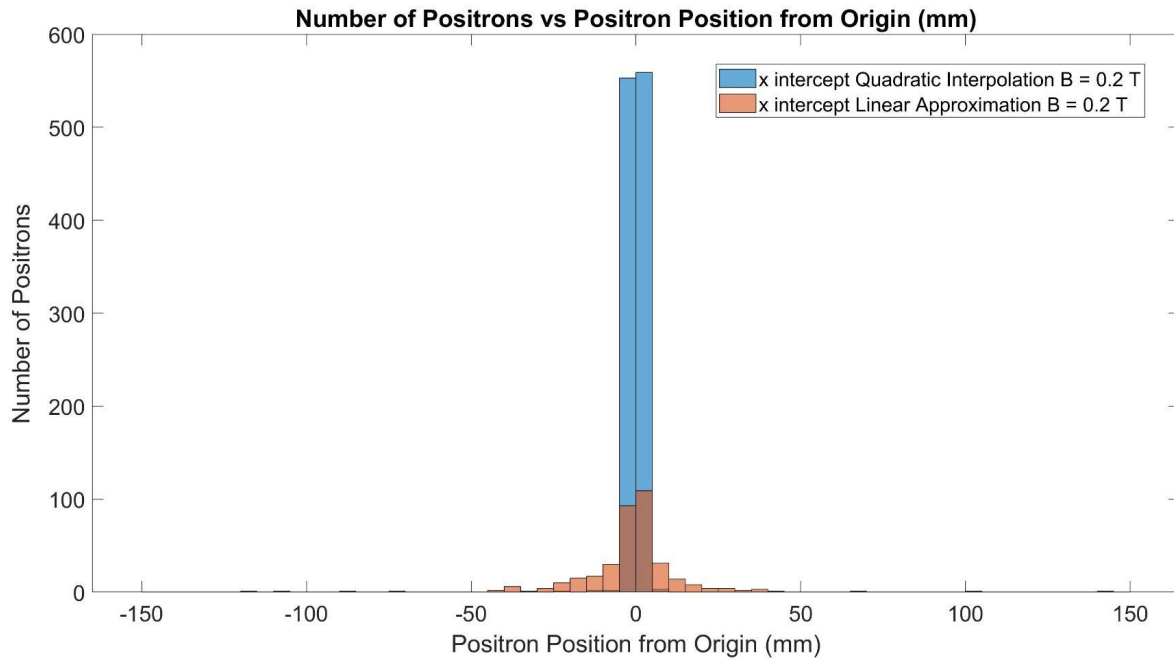
Below is the graph for Two Detectors. Here, we used linear interpolation to track back the positron's path:



Below is the graph for Three Detectors. Here we used quadratic interpolation to track back the positron's path:



When the graphs are combined, we get the following distribution:

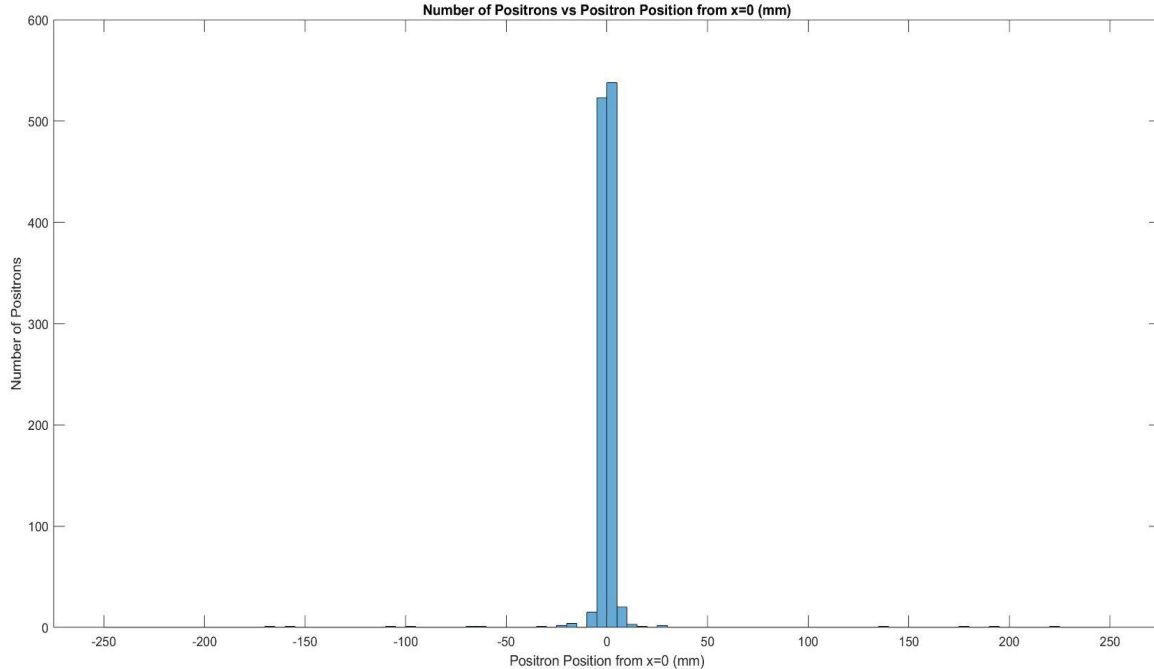


As expected, the graph is sharper for three detectors as opposed to two detectors (since quadratic interpolation is more accurate than linear interpolation).

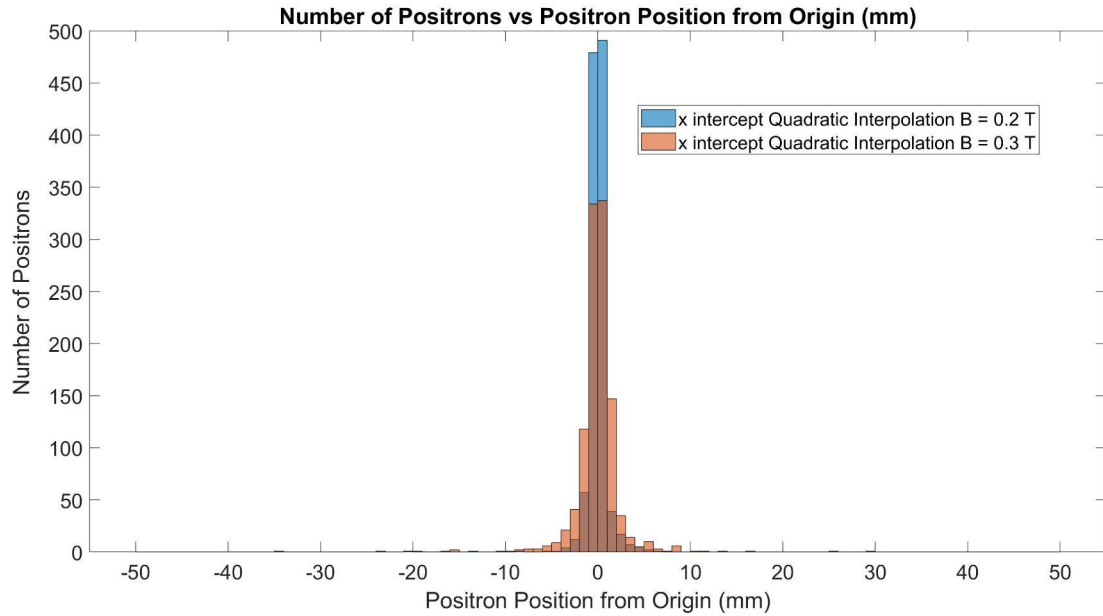
## Increasing the field to 0.3 T with Three Detectors:

If we use our quadratic interpolation method for three detectors, but for a 0.3 T magnetic field, we get the following position distribution:

3 Detectors (Quadratic Interpolation for  $B = 0.3$  T):

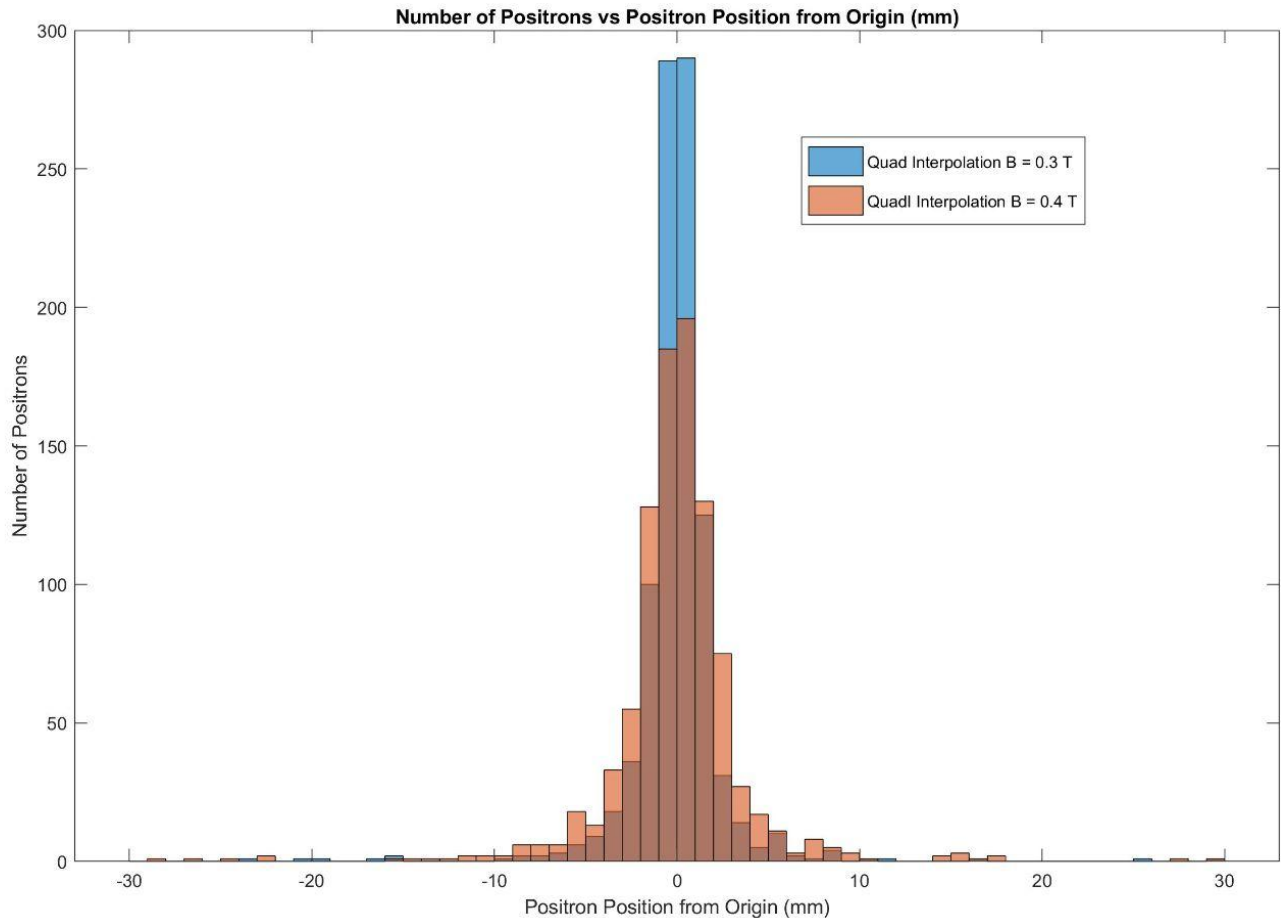


As expected, the graph for  $B = 0.3$  T is less accurate because stronger magnetic fields cause stronger path deviations for the particle thus resulting in less accurate approximations for the position.



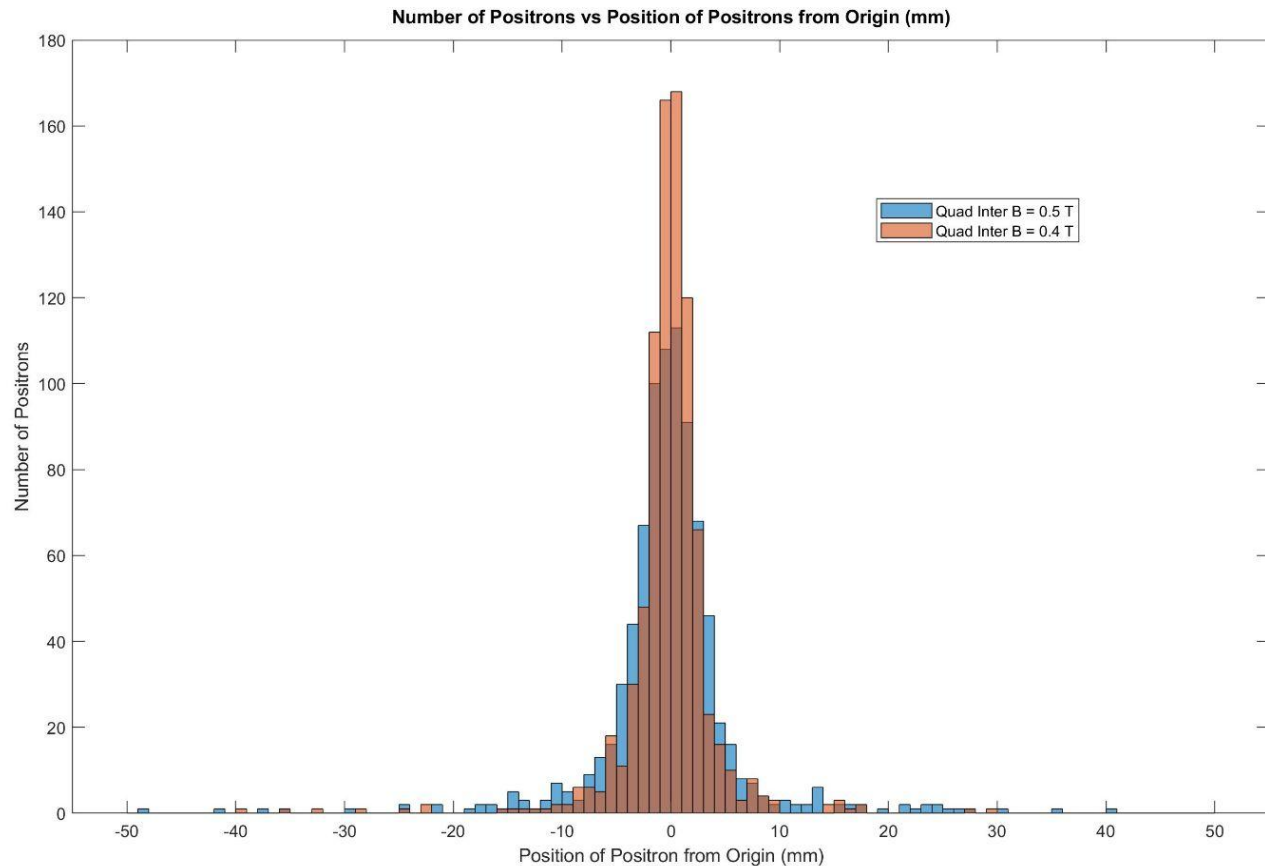
## Increasing the field to 0.4 T with Three Detectors:

If we continue using three detectors but for a 0.4 T magnetic field, we find that quadratic interpolation is less accurate than for a 0.3 T magnetic field when compared to 0.4 T magnetic field.



## Increasing the field to 0.5 T with Three Detectors:

Continuing the process of using three detectors, we increase the field by another 0.1 T to a 0.5 T magnetic field; we find that quadratic interpolation is less accurate for a 0.5 T magnetic field in comparison to a 0.4 T magnetic field. Like the previous result, this is likely due to the stronger magnetic field causing more curvature in the particle's path.



## Helical Approximation with Front Detectors:

For more information regarding our application of the helical approximation algorithm, read [this](#) link for more info (the exact same link can be found in Appendix 1).

### POST SIMULATION UPDATE:

Sometimes, the positron rotates by a specific angle between detectors which renders the algorithm inaccurate. However, there is a solution to this:

1) Lets call  $\Delta x = x_i - x_c$  and  $\Delta y = y_i - y_c$

2) We know that  $\theta = \arctan(\frac{\Delta y}{\Delta x})$

3) If  $\Delta x < 0$  (regardless of the sign of  $\Delta y$ ):

$$\theta = \theta + 180$$

Else if  $\Delta x > 0$  but  $\Delta y < 0$ :

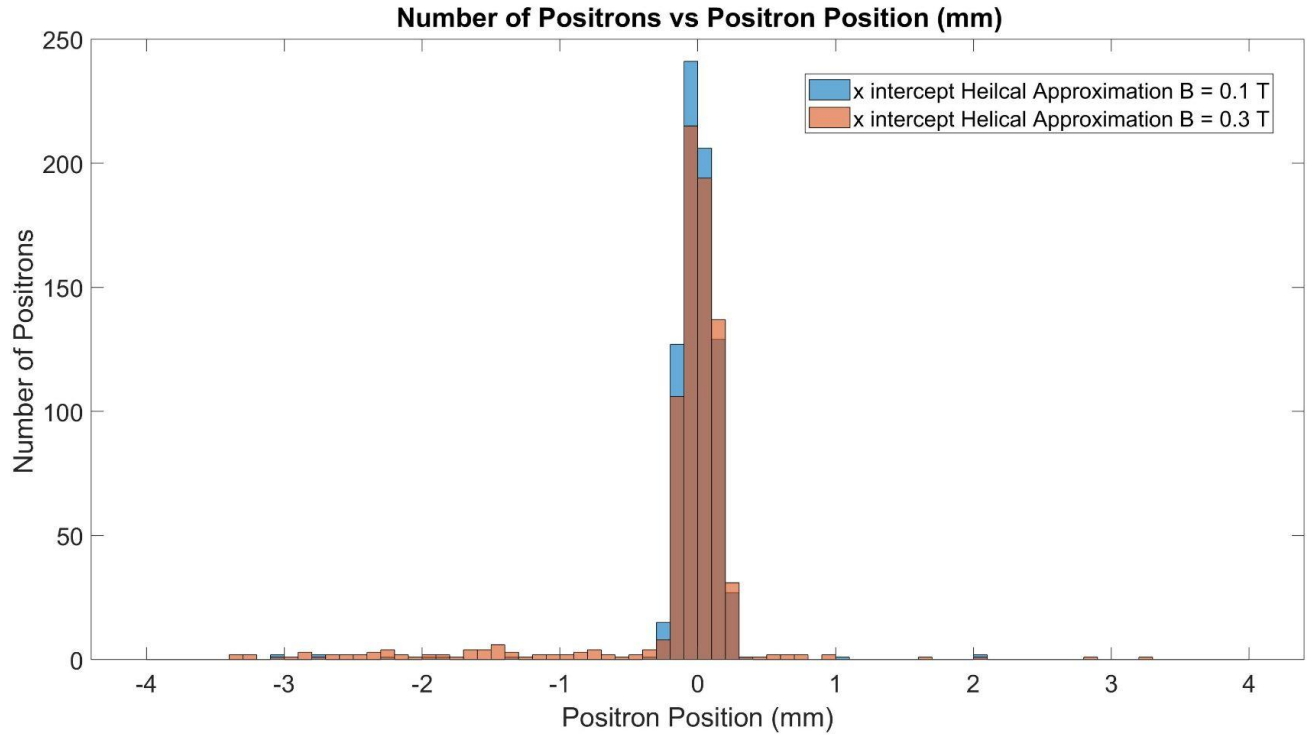
$$\theta = \theta + 360$$

In summary, what we are doing is transforming all angles into “360 degree format”, where all angles are the angle between the positive x-axis and the vector, as measured in the counterclockwise direction.

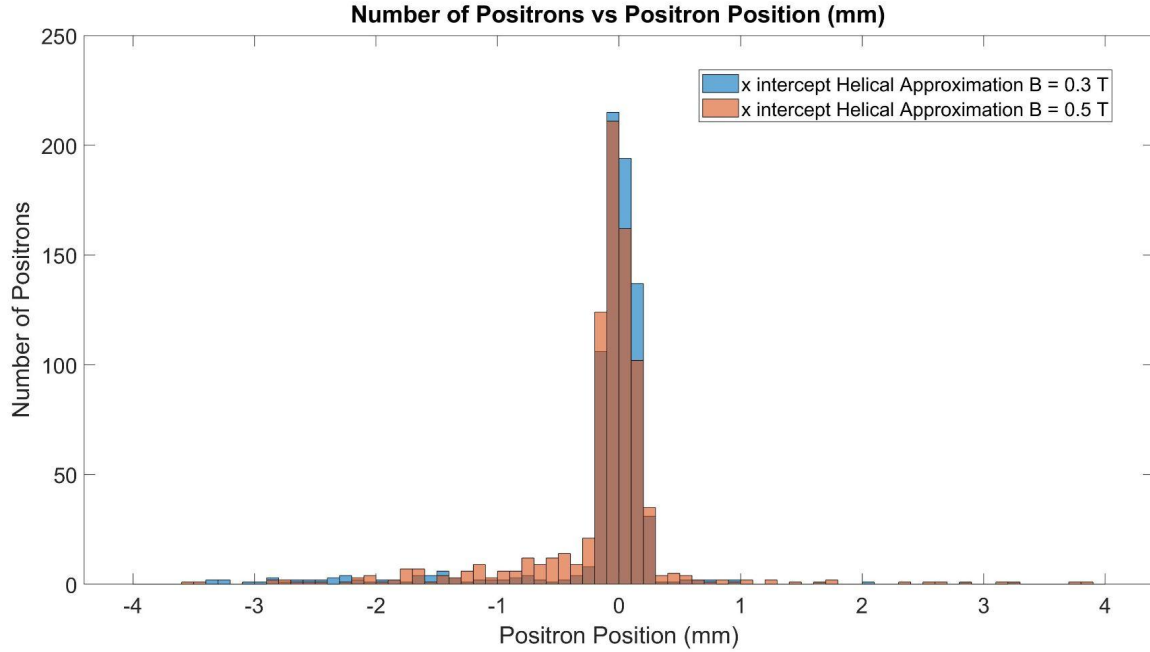
For example, before the solution above was implemented, only 771 of the 1554 values of our helical approximation algorithm in  $B = 0.3$  T were within 3 mm of the center ( $x = 0$  mm). However, after we implemented our solution, 1538 of the 1554 values were 3 mm within the center.

## Helical Approximation for $B = 0.1$ T vs $B = 0.3$ T:

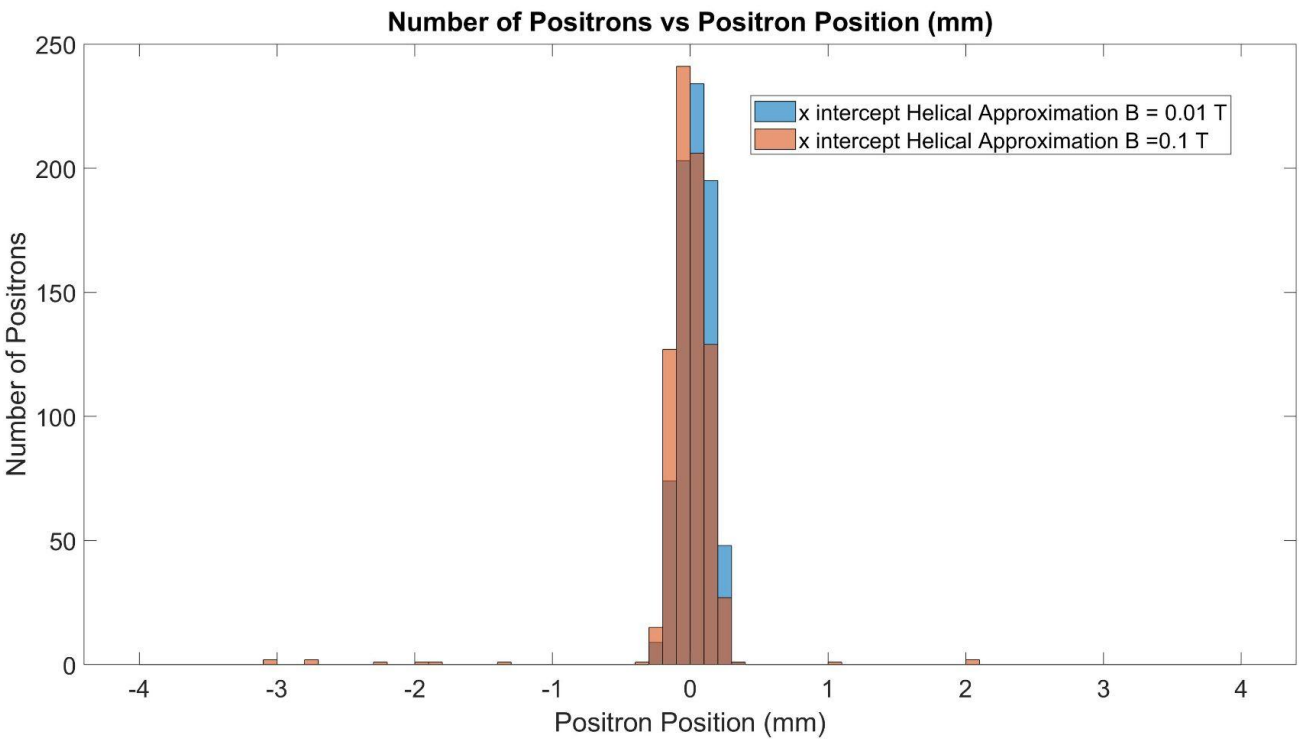
If we use the helical Approximation method as outlined in the latex document, we find the following distribution:



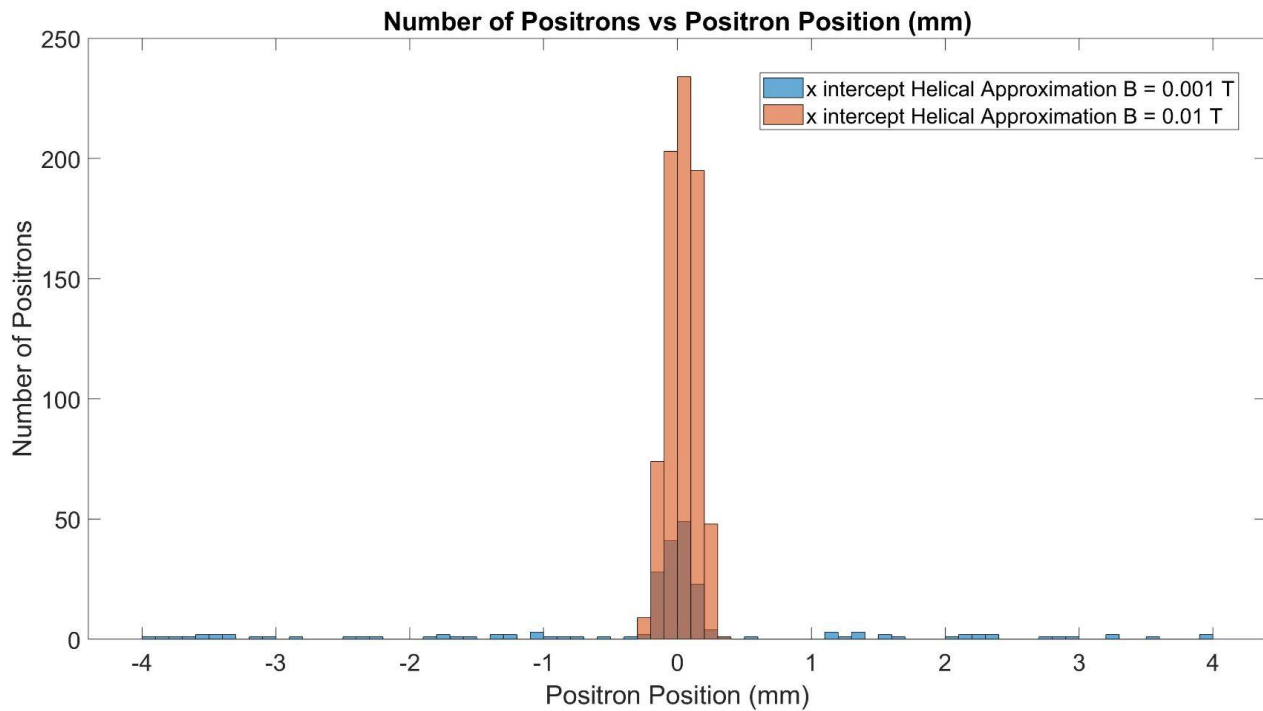
### Helical Approximation for $B=0.3$ T vs $B=0.5$ T:



### Helical Approximation for $B=0.01$ T vs $B=0.1$ T:

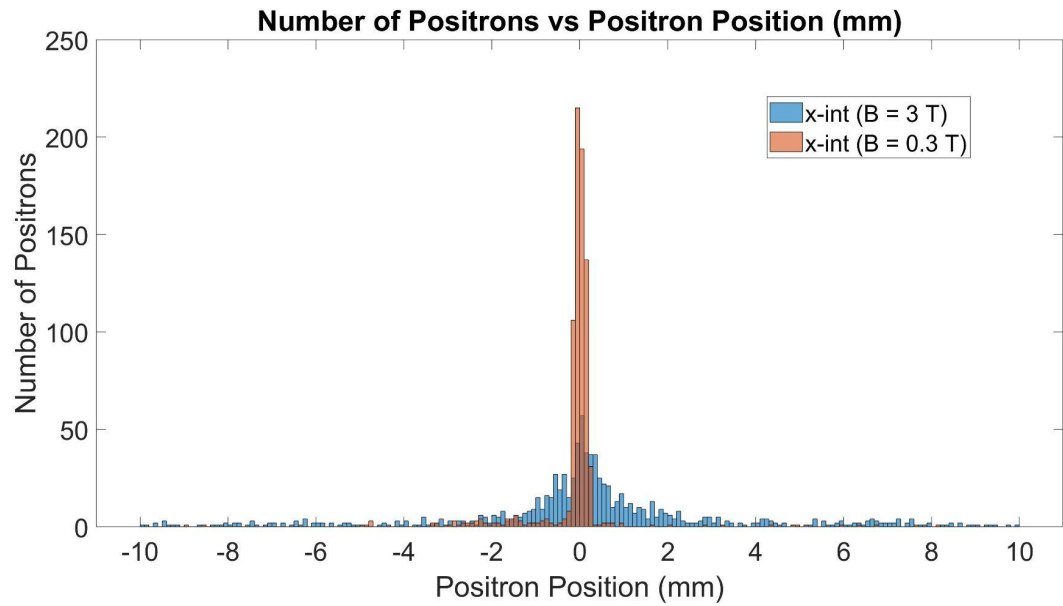


Helical Approximation for  $B=0.001$  T vs  $B=0.01$  T:



## Helical Approximation for $B=0.3$ T vs $B=3$ T:

The standard deviation of the position estimate,  $\sigma_x$ , for  $B = 3$  T is equal to 6.87 mm.

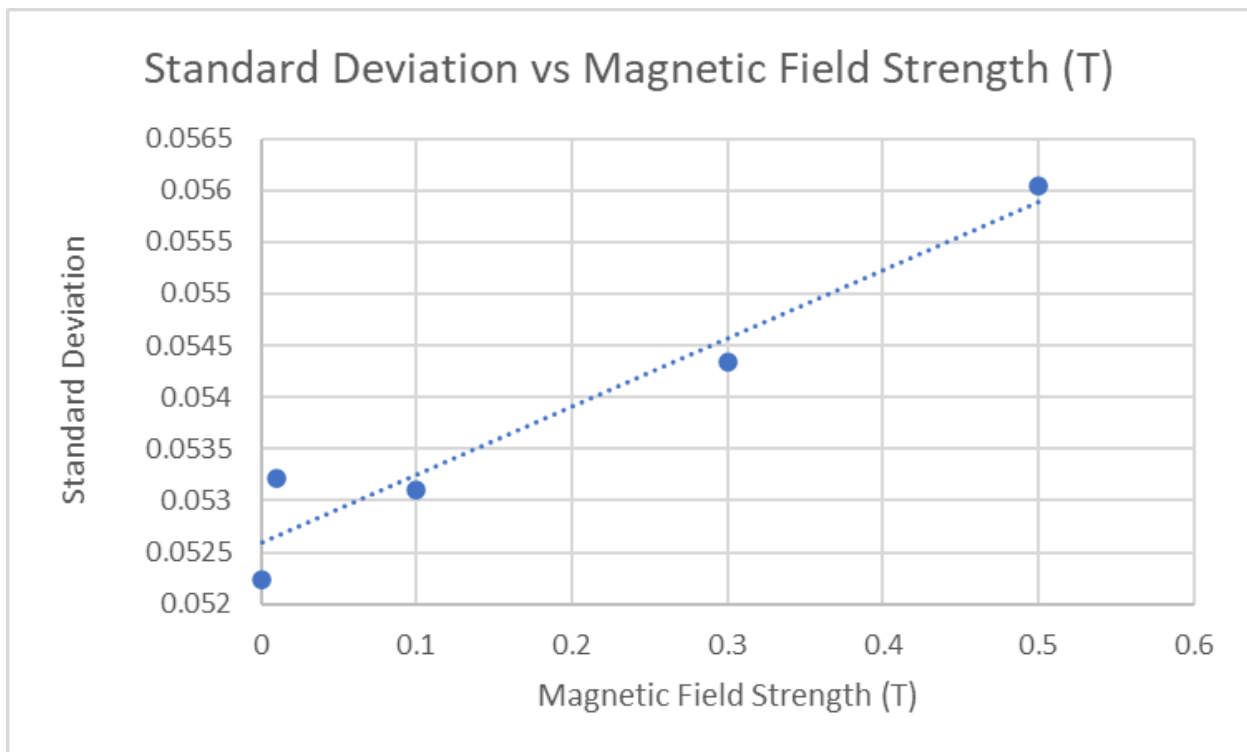


## Helical Approximation Result Analysis

If we narrow our view to near the origin (which is the point where most of the positrons are emitted from), we get an extremely accurate prediction of the origin of our positrons using the helical approximation algorithm. The algorithm is roughly as accurate for higher magnetic fields (such as 0.5 T and 0.3 T magnetic fields) when in comparison to relatively lower magnetic fields (such as a 0.01 T magnetic field). However, the algorithm does get noticeably less accurate if we go to extremely low magnetic fields (at around 0.001 T) as well as high magnetic fields (3 T).

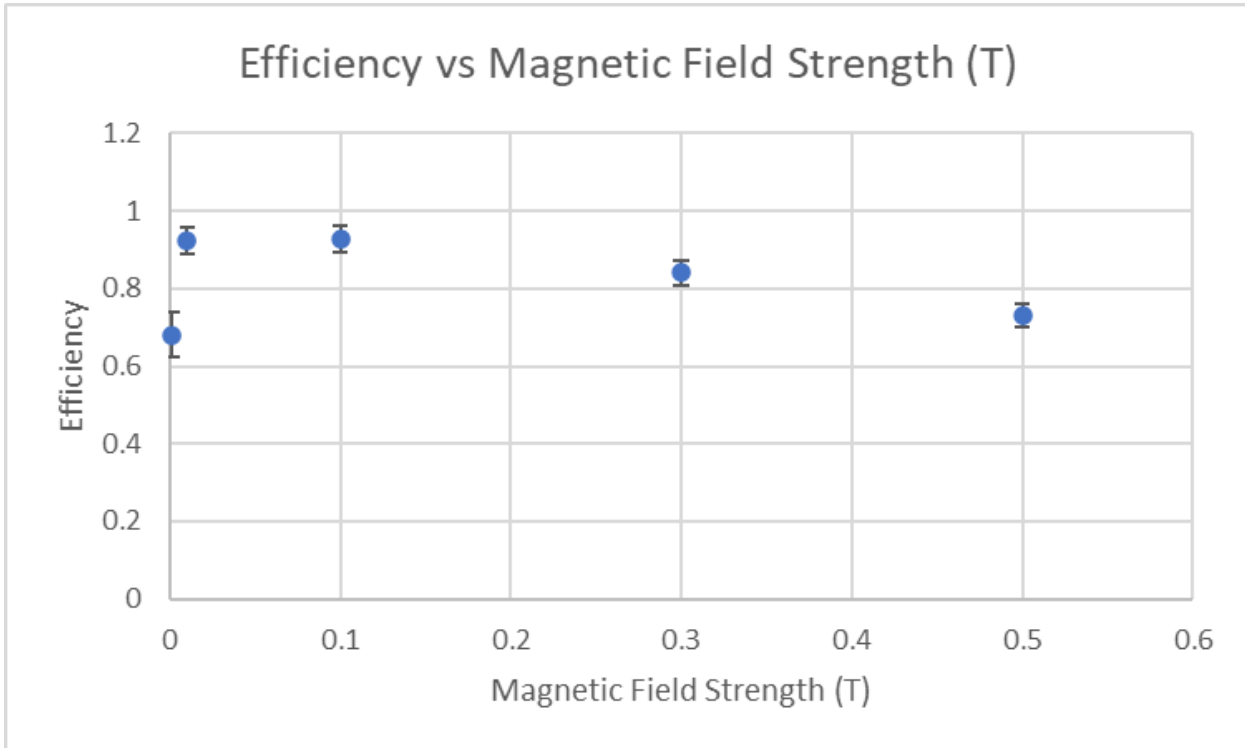
### Comparing Standard Deviation of data with magnetic field strength:

If we take data from the helical approximation method for each of the magnetic field strengths excluding 3 T (0.01 T, 0.01 T, 0.1 T, 0.3 T, 0.5 T), we see a linear relationship:



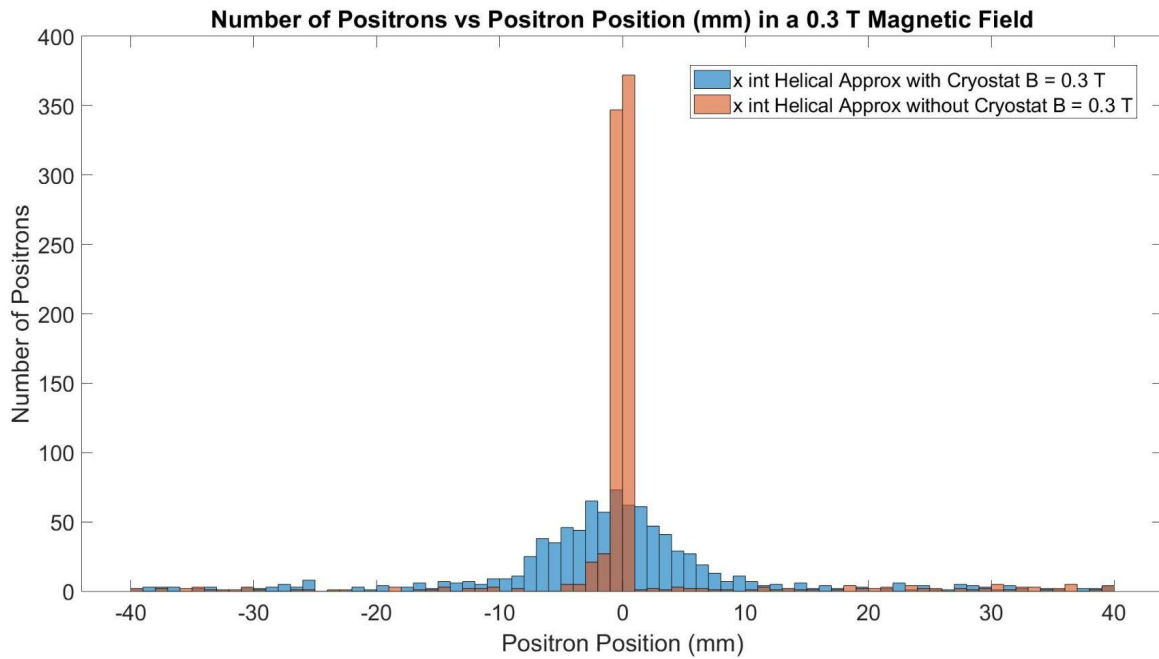
Comparing Efficiency (Counts in the 4 central bins / number of positrons detected) of data with magnetic field strength:

When we add error bars (error =  $\sqrt{N_{central}}/N_{total}$  where  $N_{central}$  is the number of positrons in the 4 central bins and  $N_{total}$  is the total number of positrons detected.)



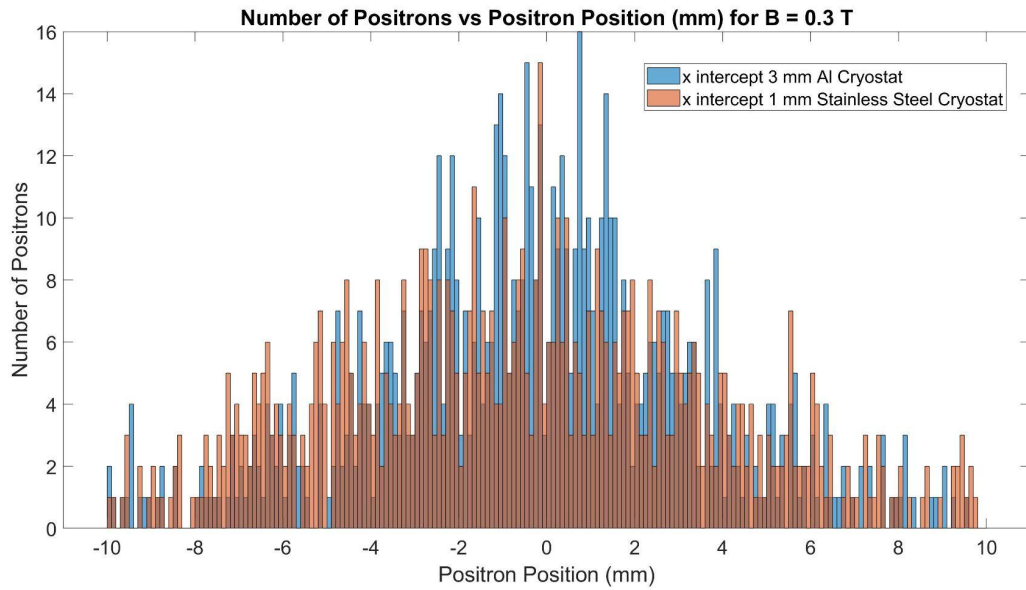
## Helical Approximation Comparison, Steel Cryostat vs No Cryostat:

If we add a 1 mm thick stainless steel cryostat to our set-up and compare it to the exact same setup but without the cryostat, we get the following:



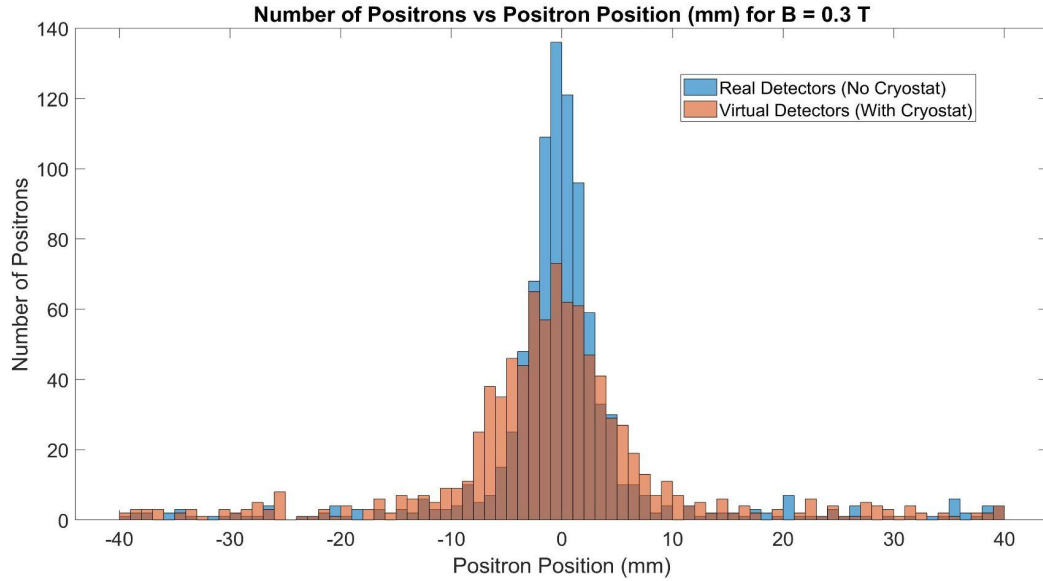
## Helical Approximation, Aluminum Cryostat vs Stainless Steel Cryostat for $B = 0.3$ T:

If we compare the helical approximation algorithms for two scenarios which are similar in every regard except for the fact that one scenario has an aluminum cryostat and the other has a steel cryostat, we get the following graph:



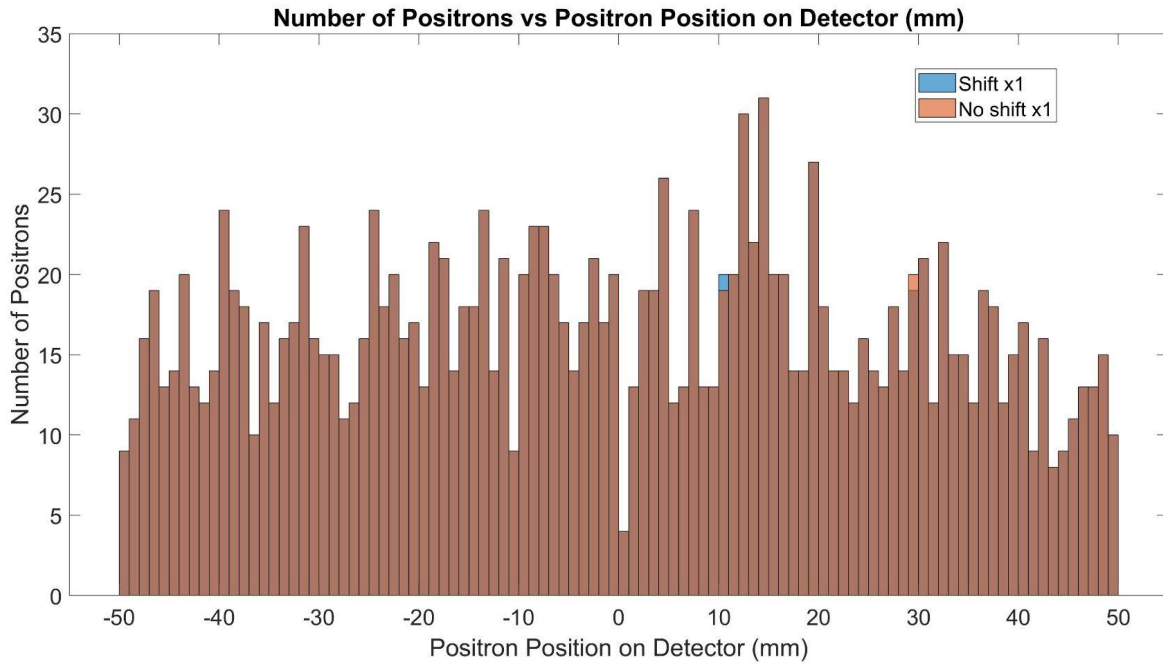
## Helical Approximation, Real detectors vs Cryostat:

If we use real detectors as opposed to virtual detectors and compare that to the scenario in which we have virtual detectors but with a cryostat, we get the following distribution below:



## Helical Approximation with target offset from the center:

If we shift the target (which the muon beam strikes) offset from the center, we get a nearly identical positron distribution for the detectors when compared to the same experiment but with no target offset. In both scenarios, out of the 1651 positrons that were detected by the first detector, only 2 deviations were spotted.



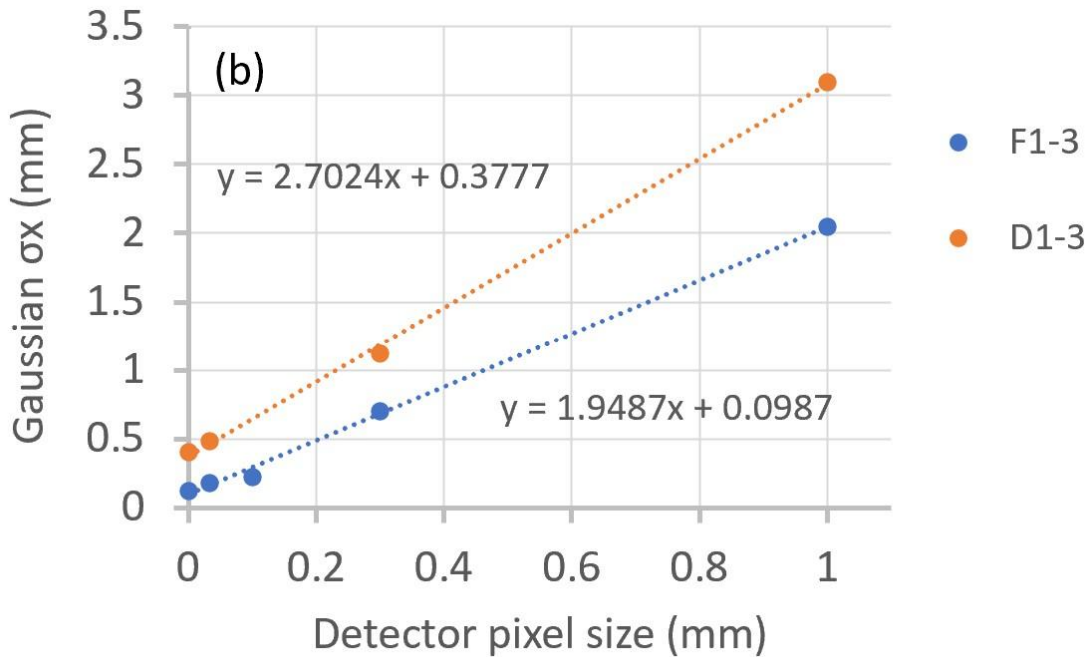
Note that the figure above does not designate the distribution of positrons after applying the helical approximation algorithms, but rather the distribution of positrons detected by the detector. Because the results of the helical approximation algorithm depend only on the distribution of positrons on the detector (as well as the detectors respective distances to the target), we find that if the distribution of the positrons for the detectors are nearly identical (keeping the same distance from the target) then the results for the helical approximation algorithm should be nearly identical.

## Graph of Standard Deviation vs Rounding number:

Let's say we round each of the  $x$  and  $y$  coordinates measured by the detector to the nearest fraction (for example; rounding to the nearest third) and then apply our herlical approximation algorithms based upon our rounded  $x$  and  $y$  values. The leftmost dot corresponds to where there is no rounding the  $x$  and  $y$  values that the detector measures. The second leftmost dot corresponds to rounding to the nearest thirtieth, the third leftost dot corresponds to rounding to

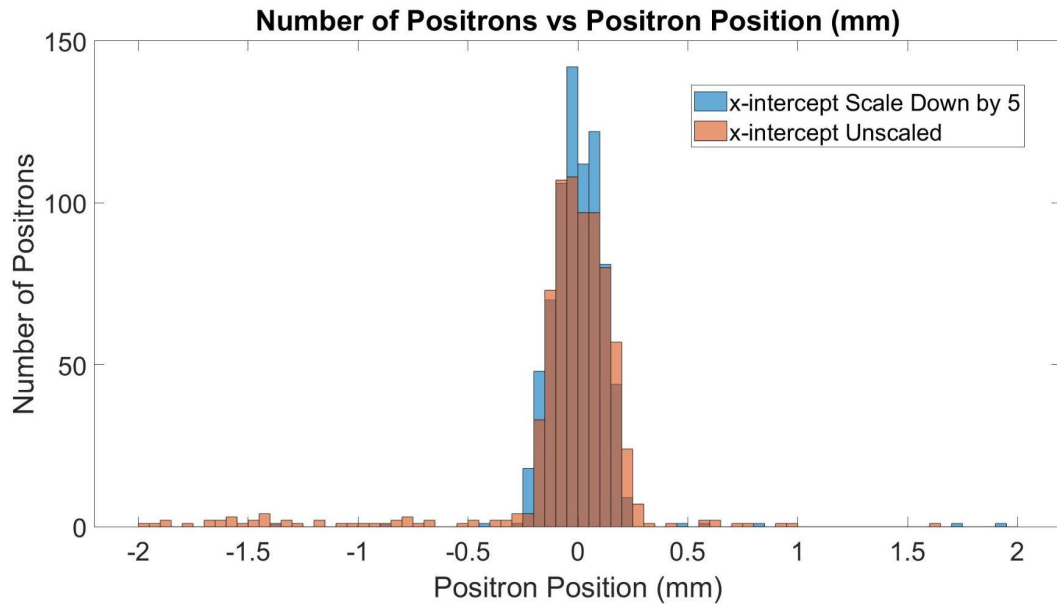
the nearest tenth, the second rightmost dot corresponds to rounding to the nearest third, and the rightmost dot corresponds to rounding to the nearest whole number.

### Standard Deviation vs Detector Pixel-Size:



## Helical Approximation but Scaled Down by 5:

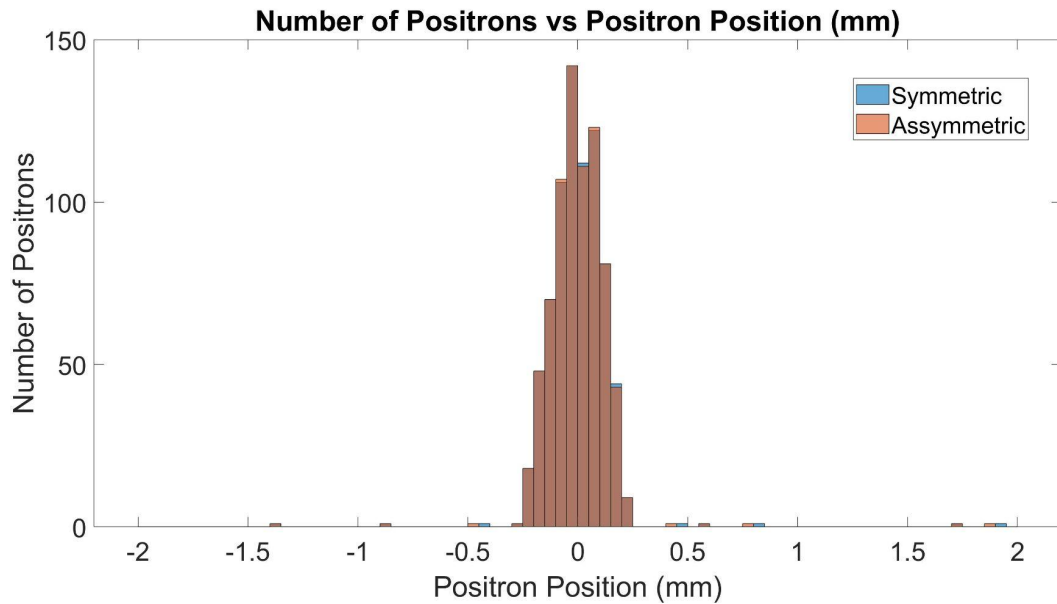
If we run our regular simulation but scale down the distances of the detectors from the target by 5 and then compare it to our usual unscaled version, we get the following graph.



If we scale down the detector distances from the target down by 5, we find that the helical approximation for the scaled down version is slightly more accurate than the unscaled version, with  $\sigma_x = 0.1148$  mm for the scaled down version.

## Symmetric Detector Placement vs Asymmetric Detector Placement for Scaled Down Scenario:

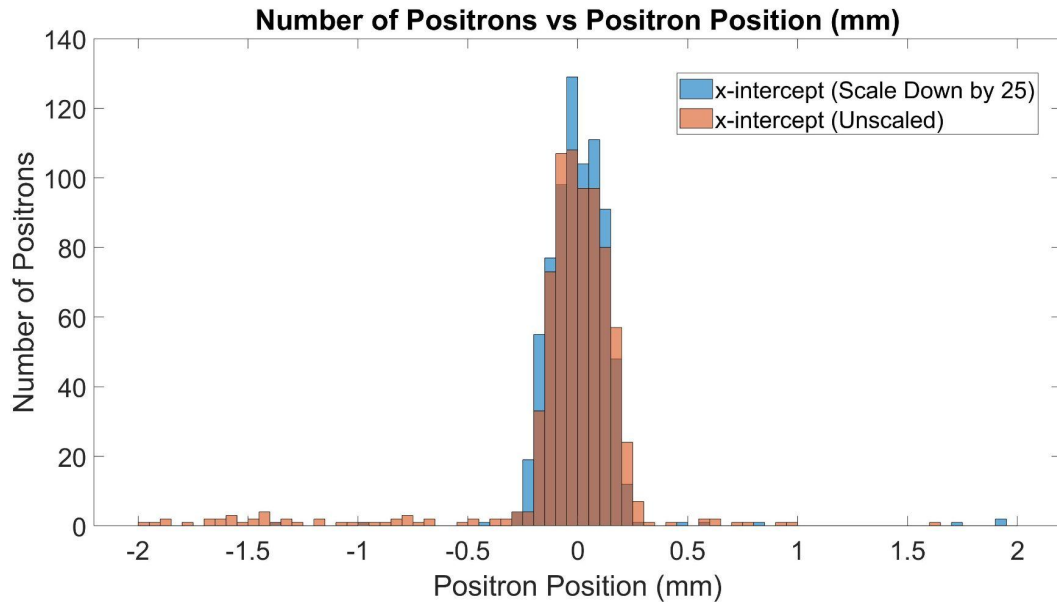
If we continue with our scaled down scenario, but move the middle detector 5 mm toward the front detector (so it is now 35 mm from the target as opposed to 30 mm) we get the following distribution when compared to the previous detector placement scenario (where it was only 30 mm from the target).



The reason why they are nearly identical is that the algorithm (after the radius and center points of the helix are calculated) only uses the z-values of the first and third detectors, and the movement of the second detector should not have an affect on the calculator of the radius and center points of the helix.

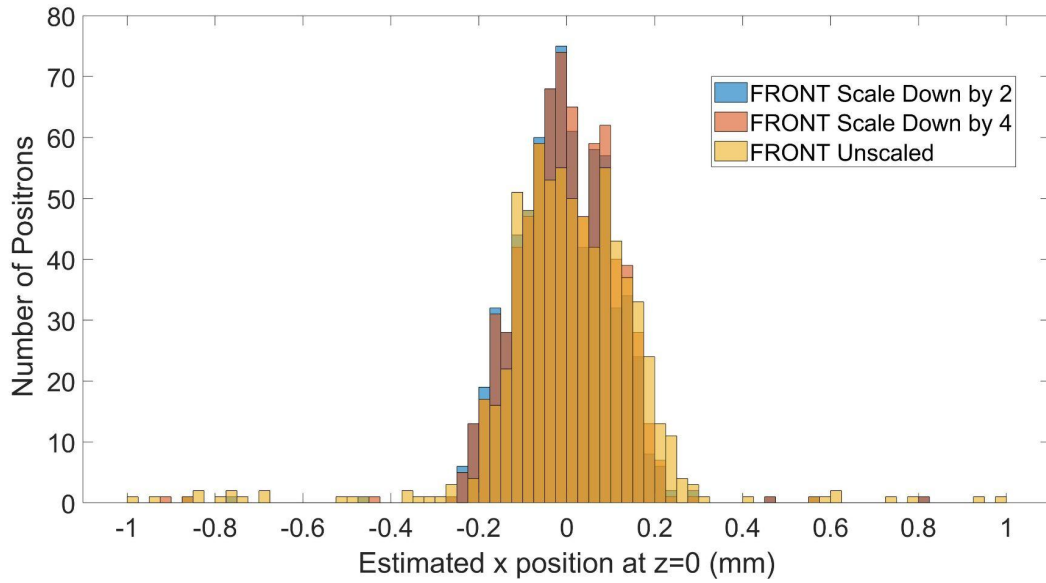
## Helical Approximation but scaled down by 25:

If we scale down our original Front-Back detector setup by 25 (while maintaining a 0.3 T magnetic field), we find that the scaled down version is about accurate as the unscaled scenario with  $\sigma_x = 0.126$  mm for the scaled scenario:



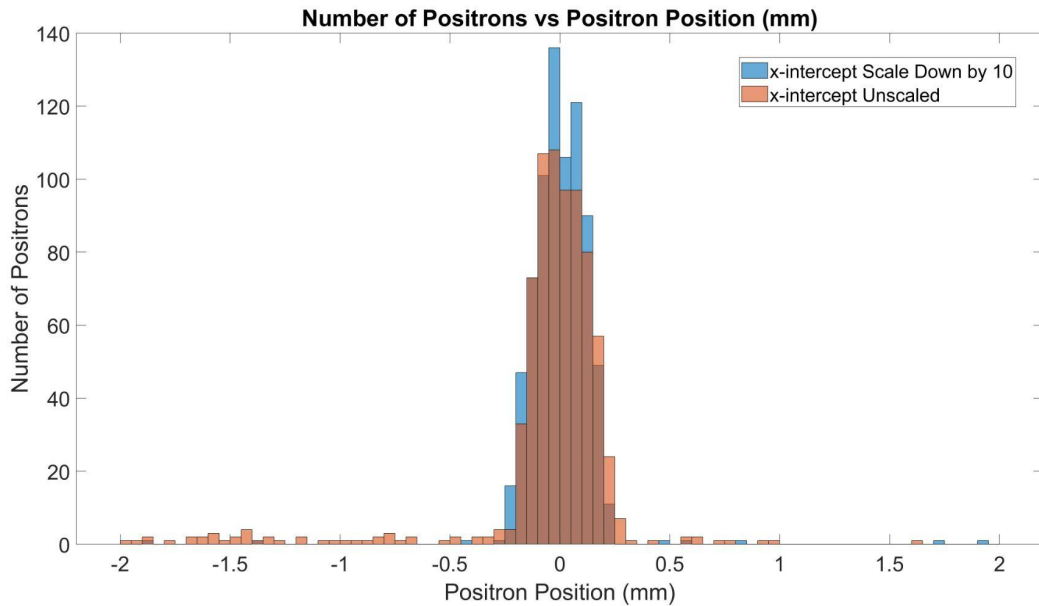
## Helical Approximation but scaled down by 2 and 4:

If we scale down our regular scenario (Uniform  $B = 0.3$  T) by 2 and 4, we find that the scaled down scenarios are slightly more accurate than the unscaled scenario, and the two scaled scenarios are very similar in accuracy, with  $\sigma_x = 0.114$  mm for the  $\frac{1}{2}$  scaled scenario and  $\sigma_x = 0.111$  mm for the  $\frac{1}{4}$  scaled scenario:



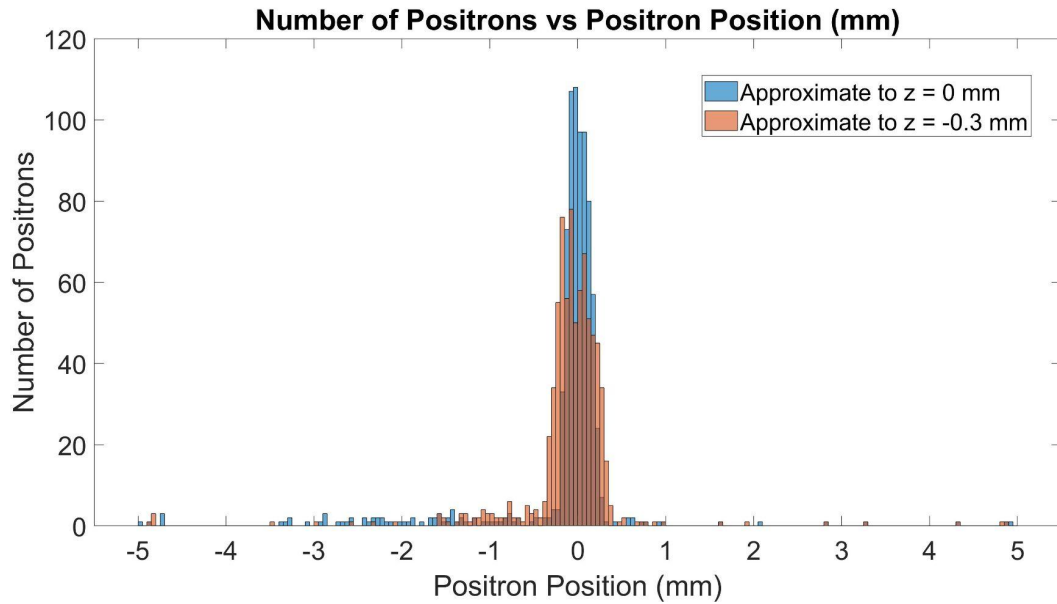
## Helical Approximation but scaled down by 10:

If we scale down our default scenario (with a uniform 0.3 T magnetic field in the z-direction) by a factor of 10, we find that  $\sigma_x = 0.1198$  mm.



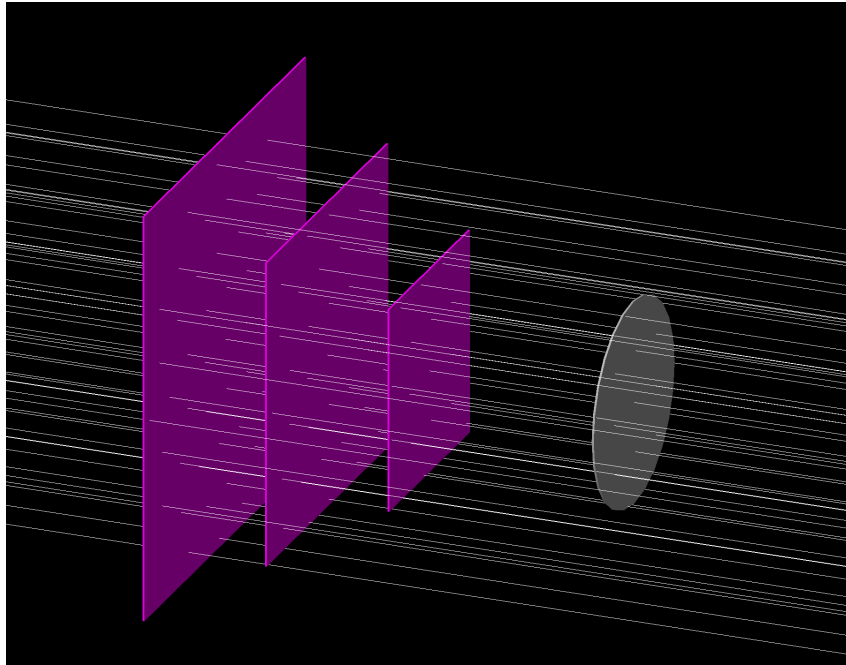
## Helical Approximation but with approximation value shifted to $z = -0.3$ :

For the simulations above, our algorithm approximated the particle's path back to  $z = 0$  mm (this is because the target is 1 mm thick, from -0.5 mm to 0.5 mm). However, if we track back to a  $z = -0.3$  mm, we find that if we approximate back to  $z = -0.3$  mm, we get less accurate results than if we approximate back to  $z=0$  mm.

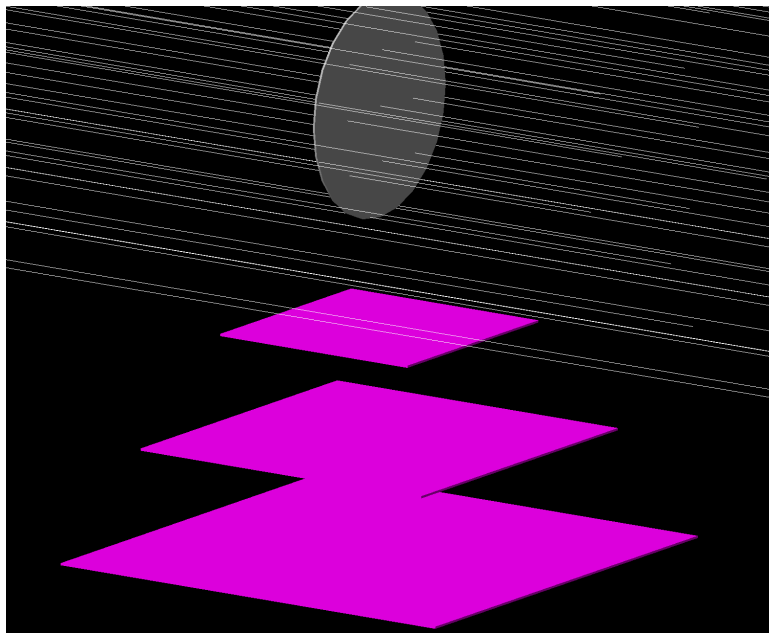


## Helical Approximation with Bottom Detectors

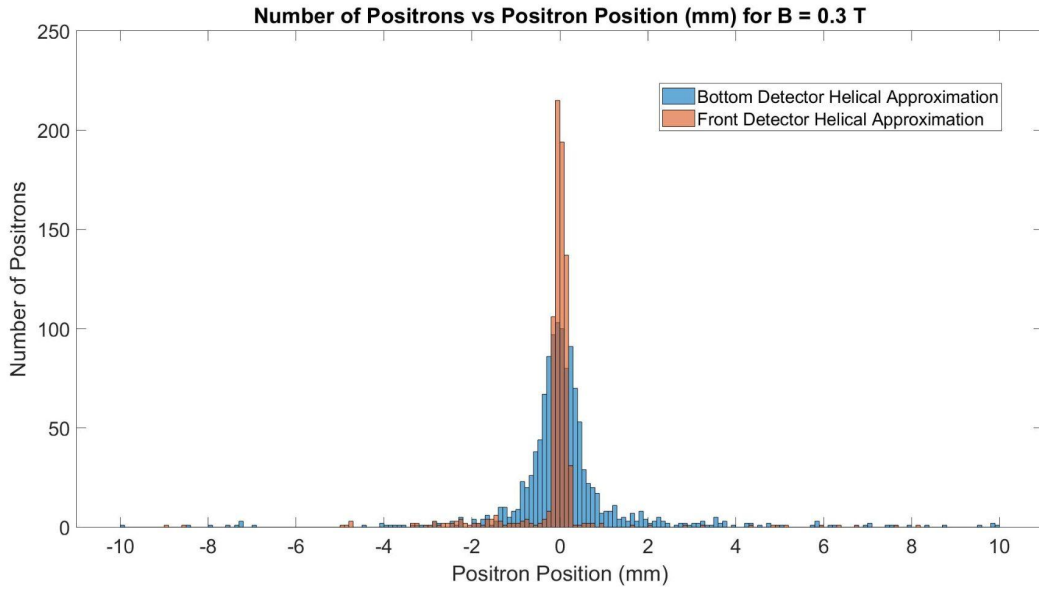
Prior to this section, every experiment we dealt with had detectors directly in line with the target and beam.



What if we rearranged the detectors to be directly below the target (as shown below) rather than in front of it?



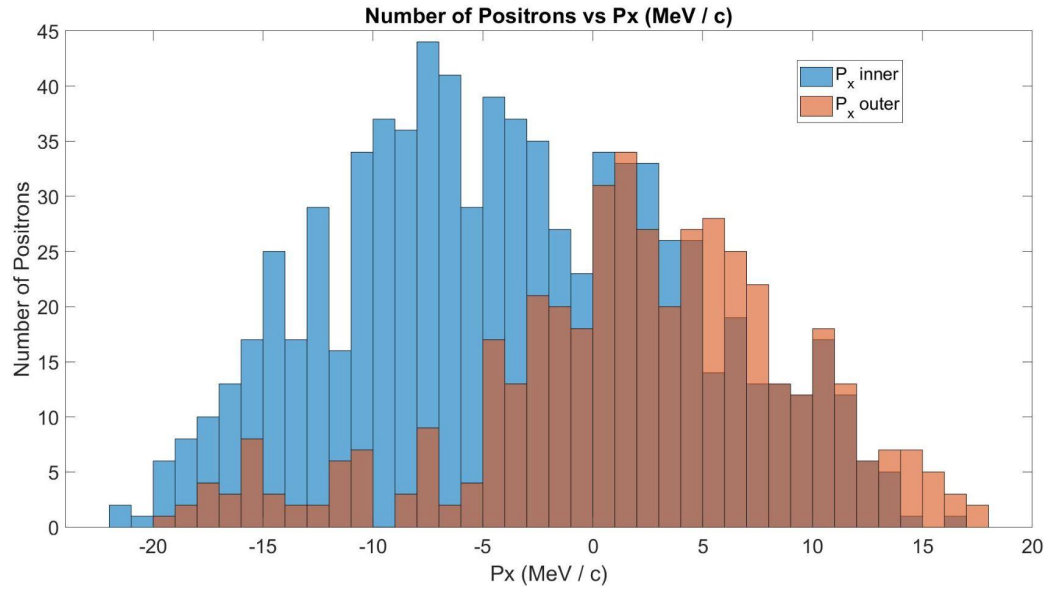
Helical Approximation with Bottom Detectors vs Front Detectors for  $B = 0.3$  T:



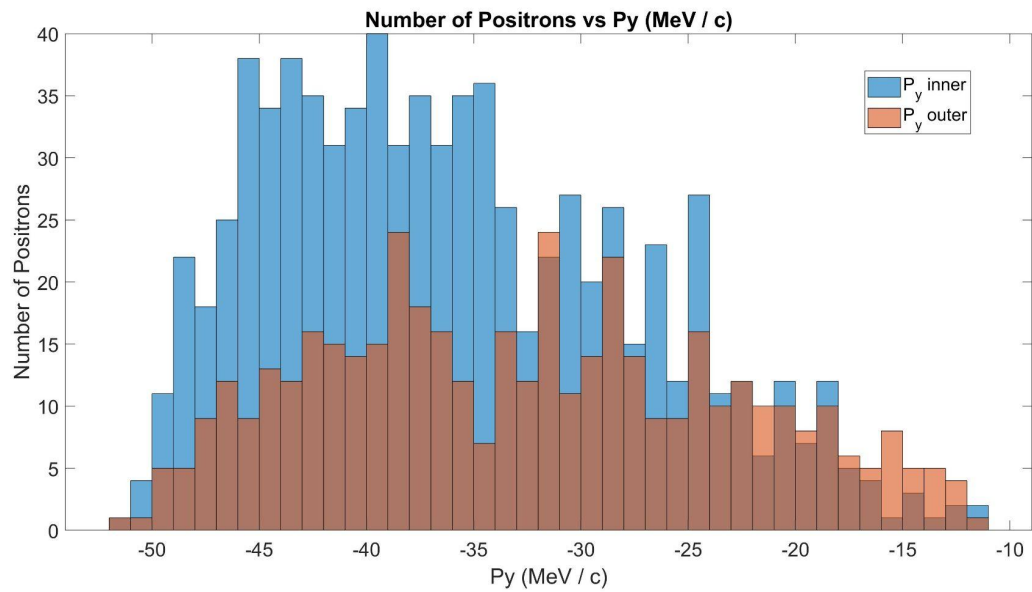
Here we see that the accuracy of the helical approximation for the front detectors is considerably more accurate than the helical approximation for the bottom detectors. However, it should also be noted that the helical approximation for the front detectors also produces lots of unrealistic values, while the helical approximation for the back detectors does not.

## Momentum Distribution for Bottom Detector Set-up (High Level Approximation):

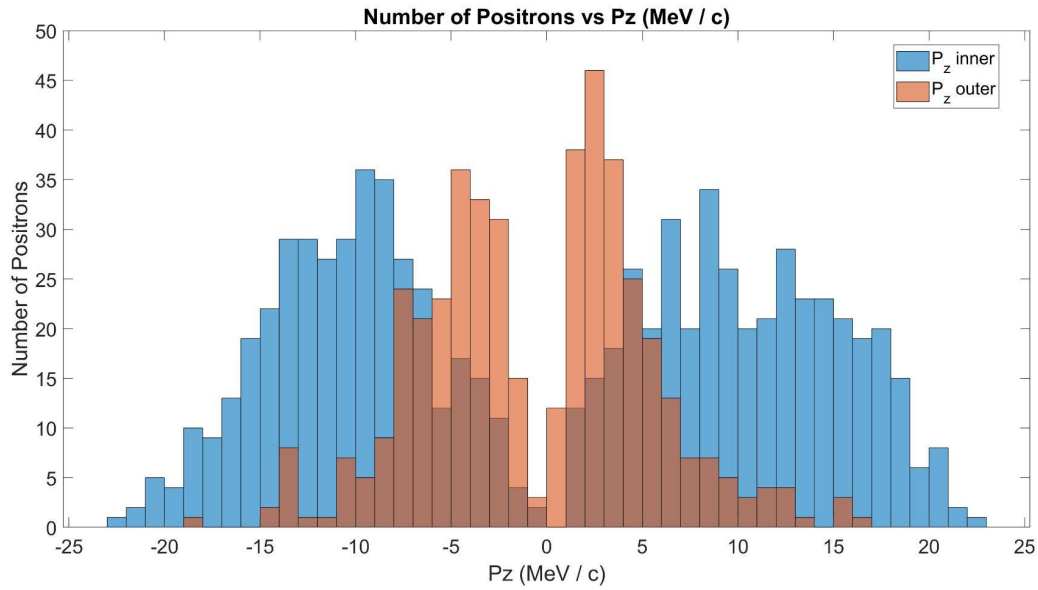
If we analyze the momentum distributions of the positions we get the following distribution of the positrons in the z direction. Here,  $P_x$  inner represents the momentum distribution of all positrons whose x-intercept with the target was calculated to be within 1.5 mm of the origin, and  $P_x$  outer represents the remaining positrons.



If we do the exact same thing for y-component of momentum, we get the following distribution:



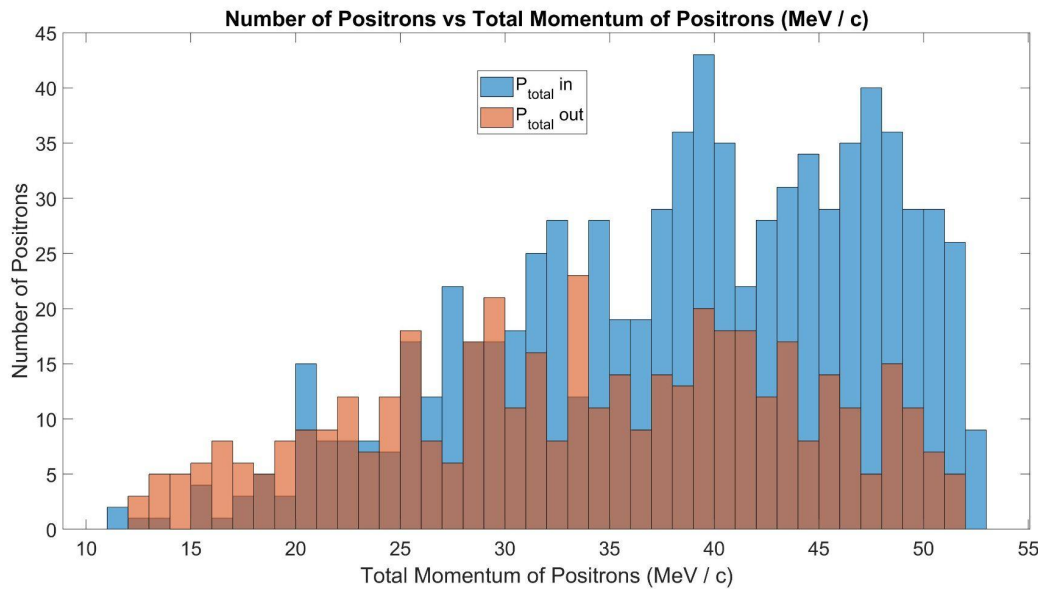
Finally, if we do it for the z-component of momentum, we get the following distribution:



Finally, if we compare the total magnitude of momentum

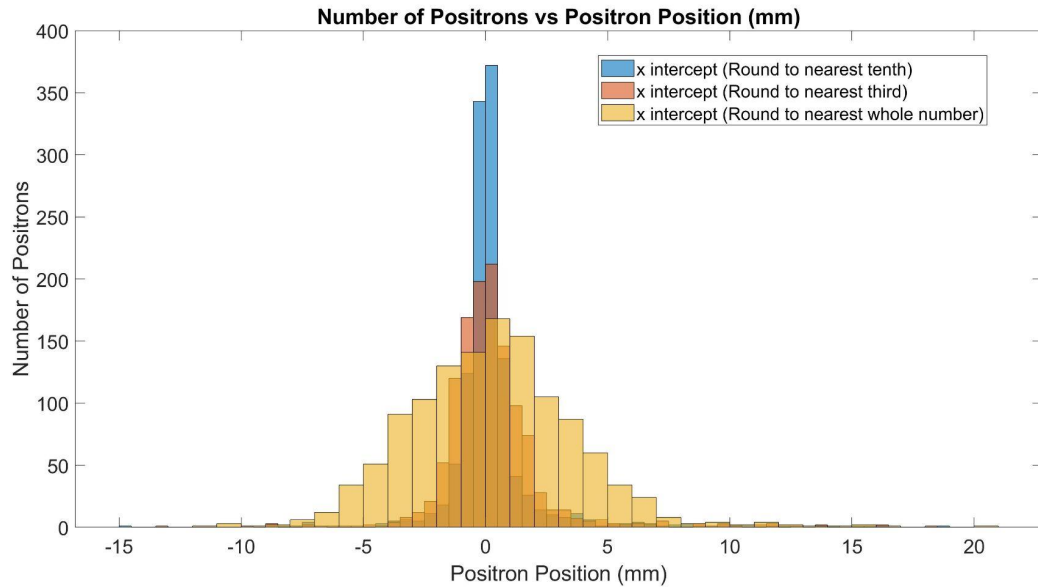
$$\|\vec{P}\| = \sqrt{(P_x)^2 + (P_y)^2 + (P_z)^2}$$

And get the following distribution:

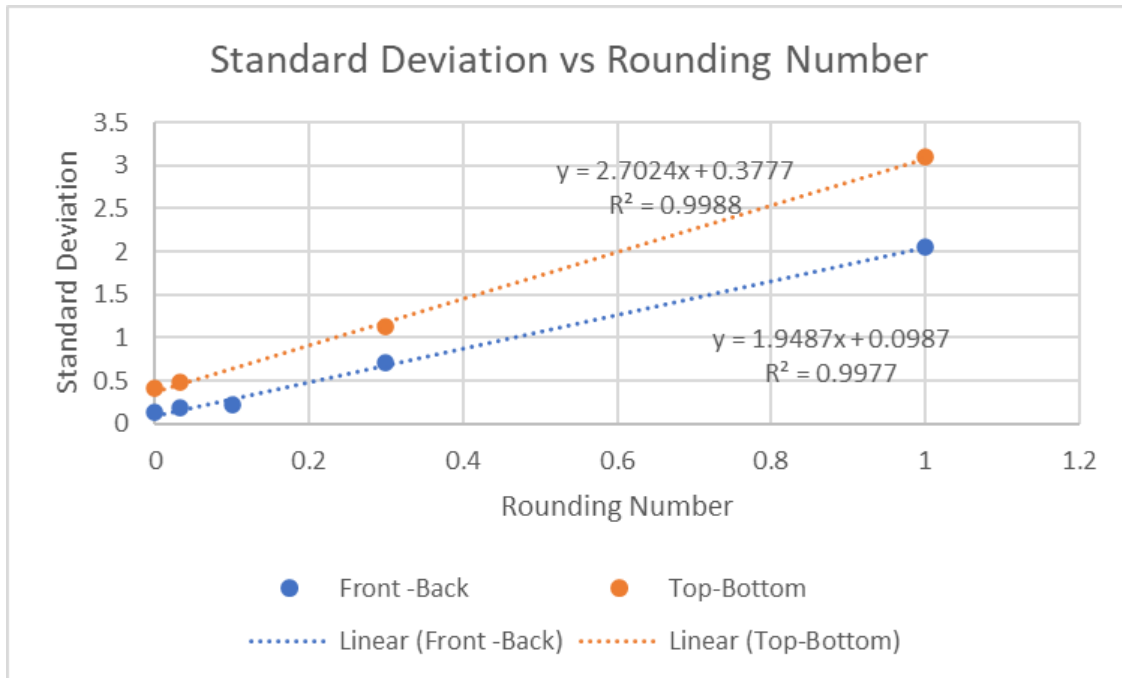


## Standard Deviation vs Rounding Number:

If we graph the our results for the helical approximation algorithm but for different rounded values of  $x$  and  $y$ , we get the following distribution for the up-down detector setup:

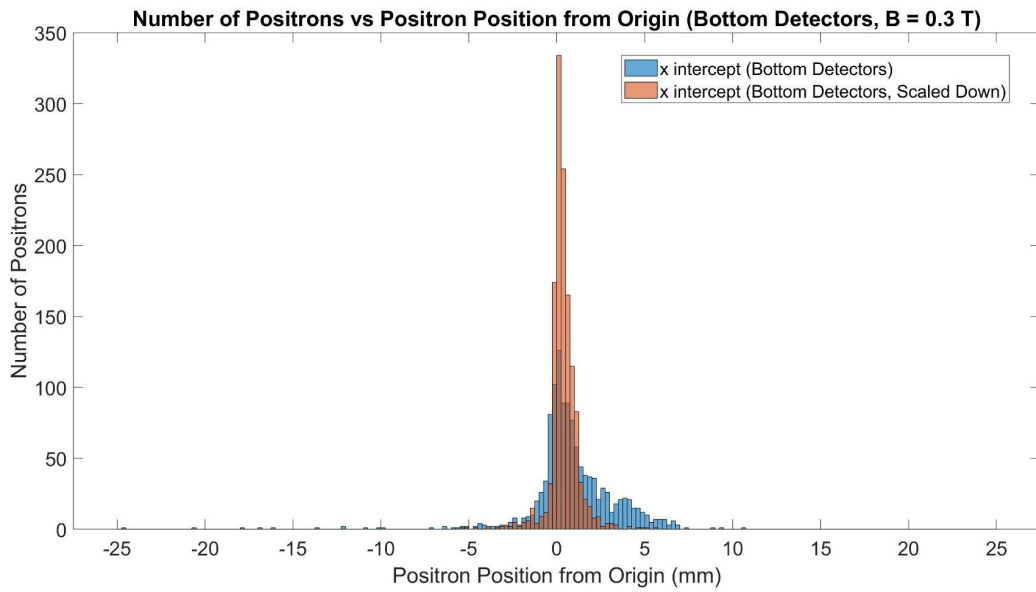


If we then compare the standard deviation as a function of the rounding number for both the front-back detector setup as well as the top-bottom detector setup, we get:



## Helical Approximation with Bottom Detectors but scaled down:

If we scale down the detectors by a factor of two (meaning each detector becomes half as wide as well as only half the distance from the target as it used to be), we get the following when comparing this so-called “scaled-down” scenario vs the original “non-scaled” scenario.



We see that the scaled down scenario is considerably more accurate than the “unscaled” scenario.

# Helical Approximation with Solenoids:

## Front-Back Setup (Large Current):

We can do a similar simulation as before but we add six solenoids to create a more realistic simulation. The code for the following simulation is below:

```

param set deltaT=0.01
param set maxStep=1.0

physics QGSP_BIC_EMZ
setdecay mu+ lifetime=2197 e+,nu_e,anti_nu_mu=1.0

beam gaussian polarization=0,0,-1 particle=mu+ meanMomentum=30
nEvents=25000 z=-1250

particlecolor mu+=0,0,1 e+=1,0,0, nu_e=0.3,0.3,0.3,
anti_nu_mu=0.5,0,0.5

trackcuts keep=mu+,e+,nu_e,anti_nu_mu kineticEnergyCut=0

material C A=12.011 Z=6 density=2

coil C innerRadius=150 outerRadius=160 length=10
solenoid S coil=C current=119360 color=1,0,0,0.3

tubs Target1 outerRadius=10 material=C length=1 color=0.9,0.9,0.9

virtualdetector Detclose width=100 height=100 length=1 color=1,0,1
require='PDGid==11'

virtualdetector Detmid width=150 height=150 length=1 color=1,0,1
require='PDGid==11'

virtualdetector Detfar width=200 height=200 length=1 color=1,0,1
require='PDGid==11'

place Target1 z=0

place Detclose z=100 rename=CloseFrontDetector
place Detmid z=150 rename=MidFrontDetector
place Detfar z=200 rename=FarFrontDetector

place S z=-100

```

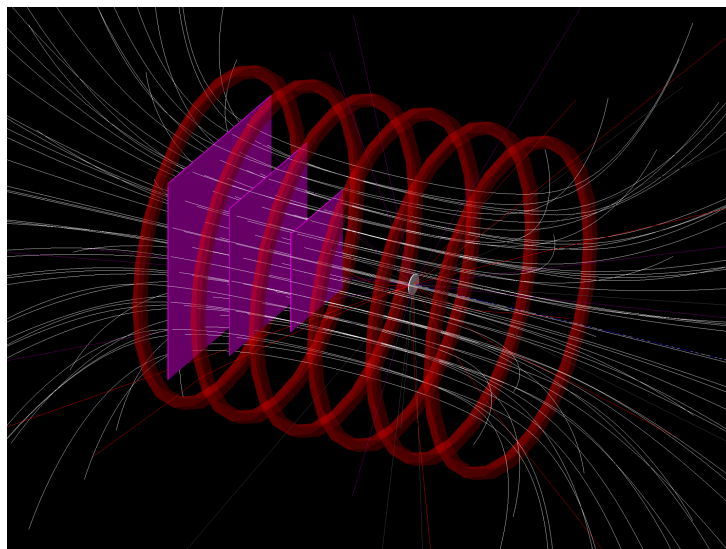
```

place S z=-40
place S z=20
place S z=80
place S z=140
place S z=200

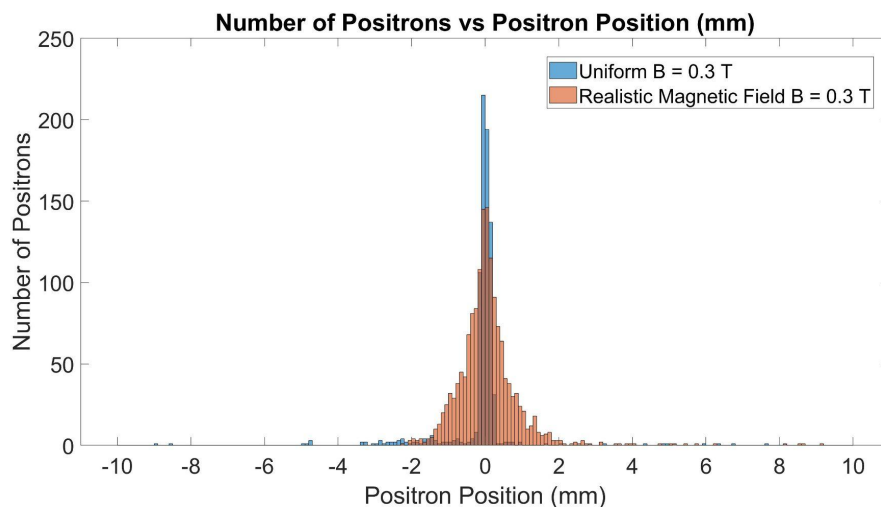
fieldlines exit=1 center=0,0,0 nLines=100

```

The setup for the simulation is visualized below:



If we compare the accuracy of our helical approximation algorithm with a uniform magnetic field (such as in previous sections) to a scenario in which we generate our field based on solenoids, we find that having a uniform magnetic field leads to more accurate results. In fact, the standard deviation of the positron distribution with the realistic magnetic field is 0.4658.

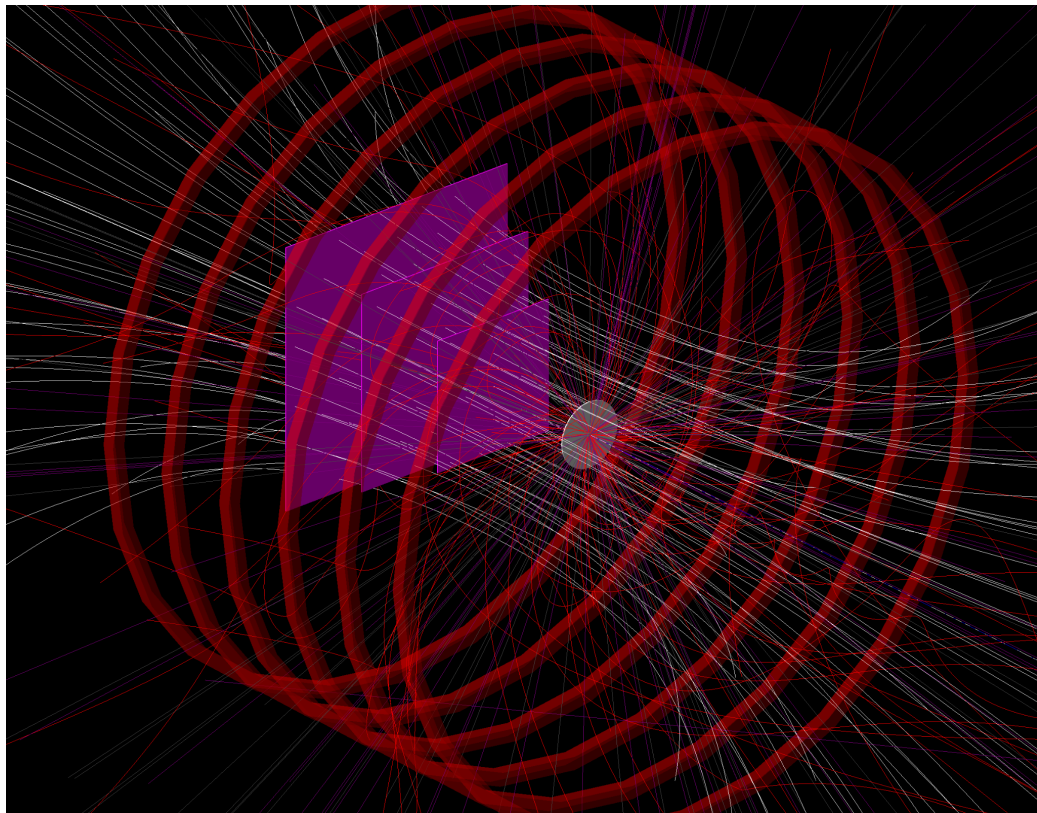


## Front-Back Setup (Small Current):

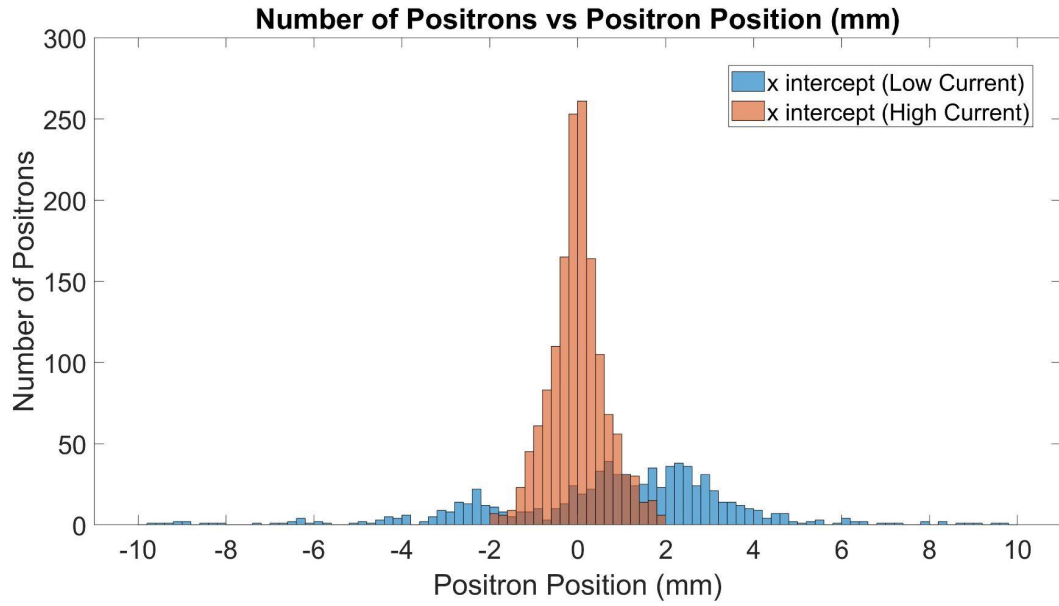
If we carry out a similar experiment as before, but we substantially decrease the current, the radius of the helical paths of the positrons will increase. This is because the centripetal force on the positrons is weaker as the magnetic force on them is weaker, which is consistent with the formula:

$$F_{Magnetic} = q(\vec{v}_{e^+} \times \vec{B})$$

The setup for the simulation is visualized below:

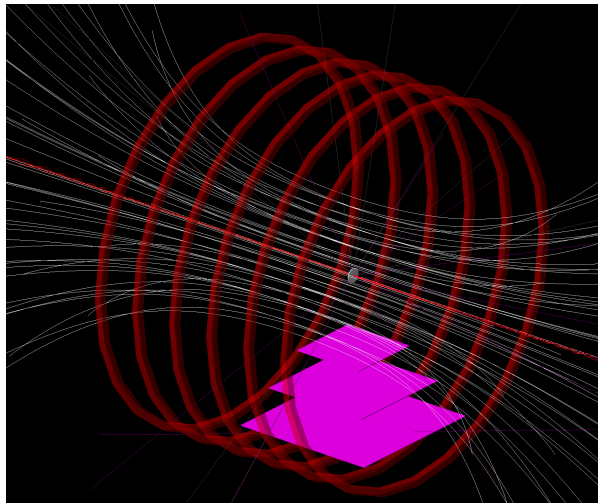


If we analyze the positron distribution between the high current and low current scenarios we see that the setup with a higher current leads to a more accurate result:

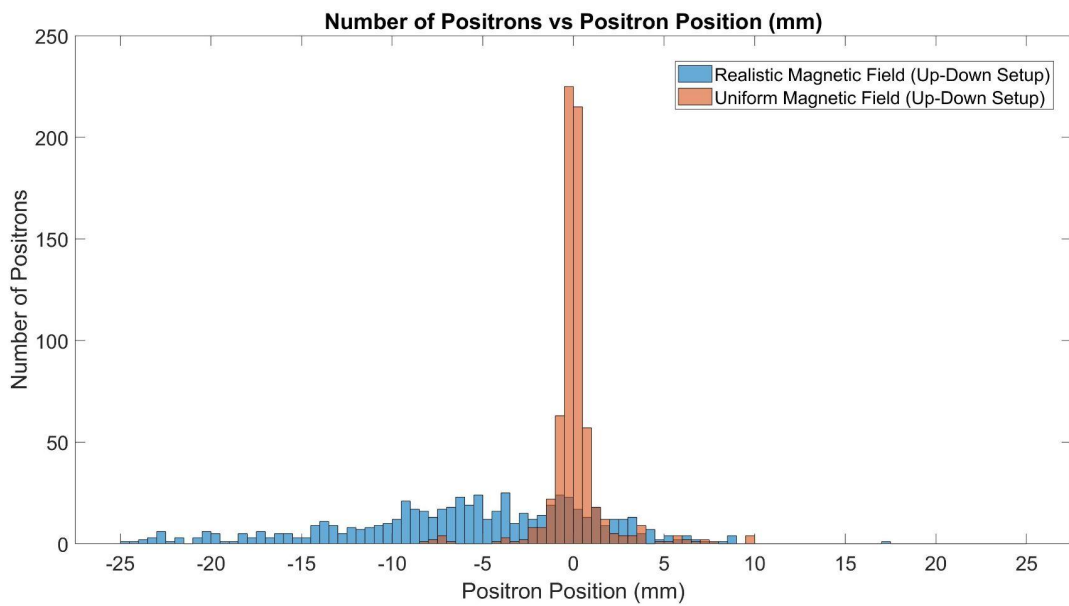


## Up-Down Setup:

We can do a similar experiment with the solenoids but with the up-down setup (as shown below), we can also decrease the current to 600 A in order to increase the number of positrons detected by the bottom detectors.



As shown in the image below, if we add a magnetic field, we find that our helical approximation algorithm is substantially less accurate for a realistic magnetic field, when compared to the same setup but with a uniform magnetic field.



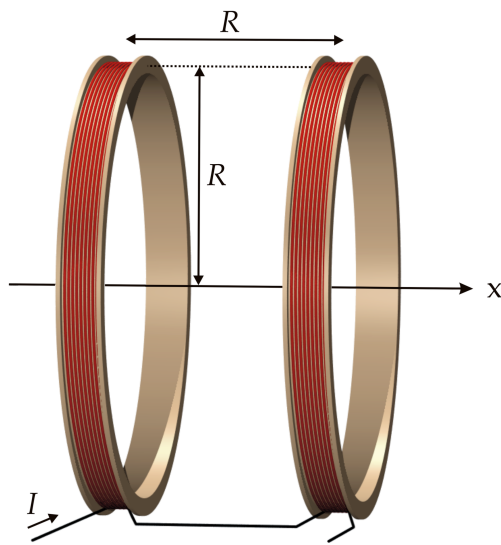
## Helical Approximation with Ideal Helmholtz Coil:

### Front-Back Setup:

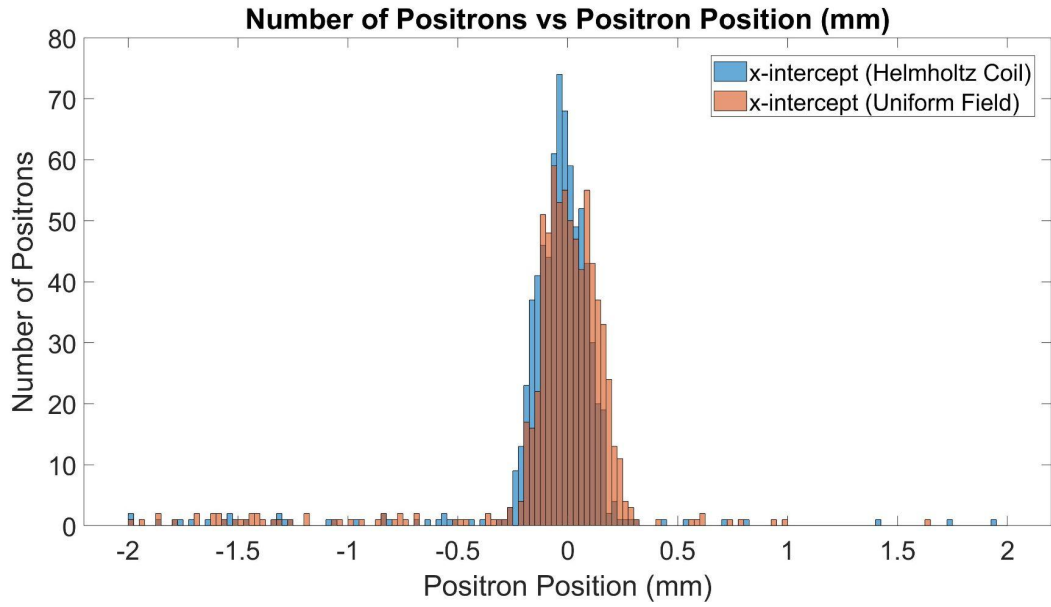
Instead of solenoids, what if we added a helmholtz coil? A helmholtz coil is a device consisting of two coils that generate an approximately uniform magnetic field across the axes of the two coils as shown below:

$$B_{\text{helmholtz}} = \left(\frac{4}{5}\right)^{\frac{3}{2}} \mu_0 n I / R$$

Where  $I$  is the current (in A),  $n$  is the number of turns per coil,  $\mu_0 = 4\pi * 10^{-7}$  (in T \* m/A), and  $R$  is the radius of each coil (in m).

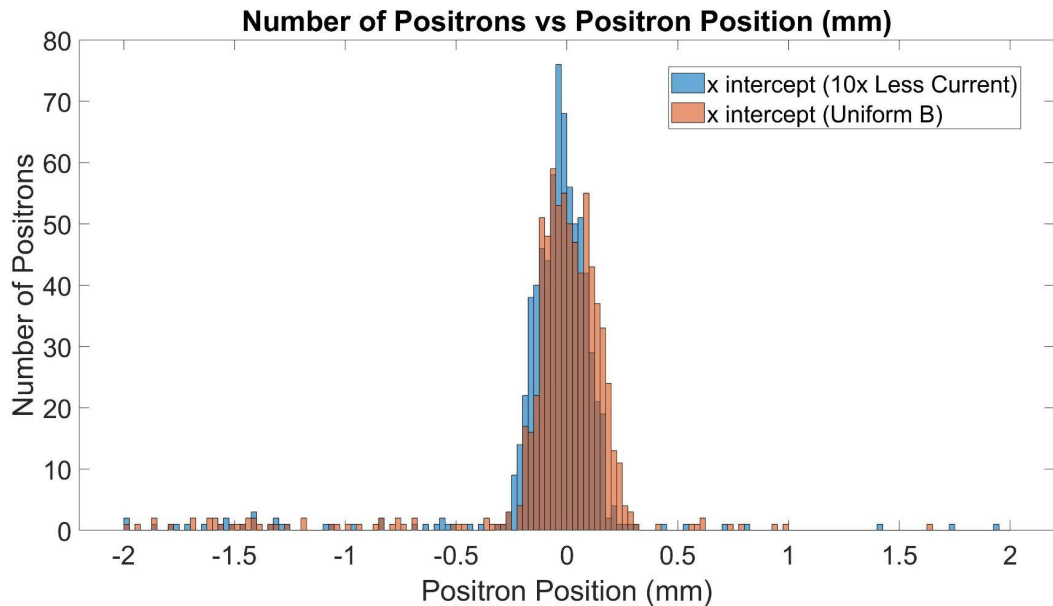


If we compare the accuracy of our helical approximation algorithm for the helmholtz coil setup and compare it to a similar setup but with a uniform 0.3 T magnetic field, we find that the helical approximation algorithm for the helmholtz setup is more accurate. However, it is likely that in the helmholtz coil simulation, a magnetic field greater than 0.3 T was produced within the coil, leading to a more accurate results (since greater magnetic fields produce helical trajectories of a smaller radius, which in turn reduces the absolute error in our approximation).



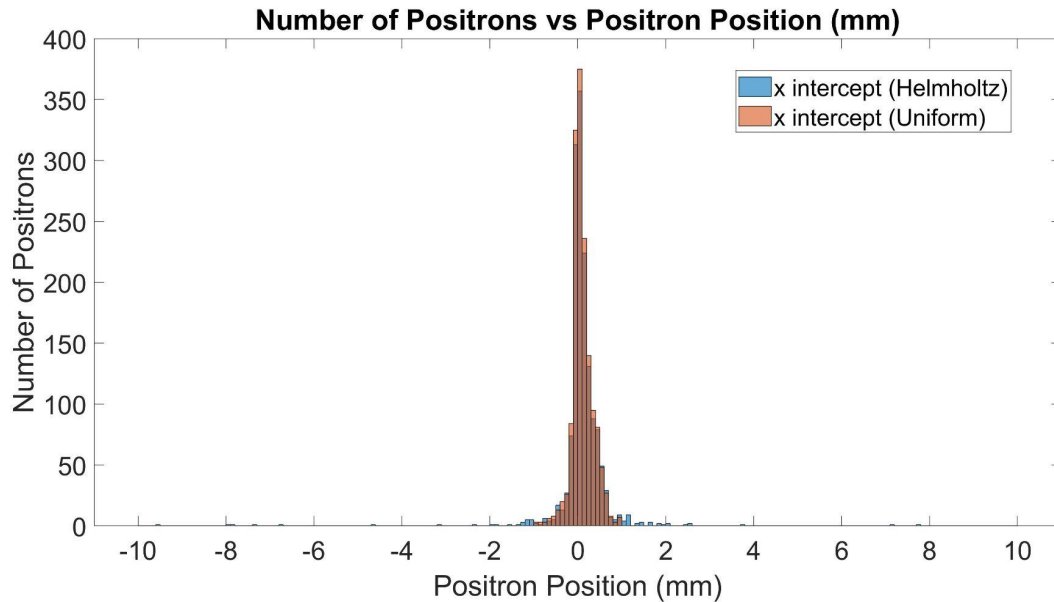
### Front-Back Setup (10x Less Current as before):

If we do the exact same simulation as before, but decrease the amount of current flowing through the coil by a factor of 10, we get the following distribution:



## Up-Down Setup:

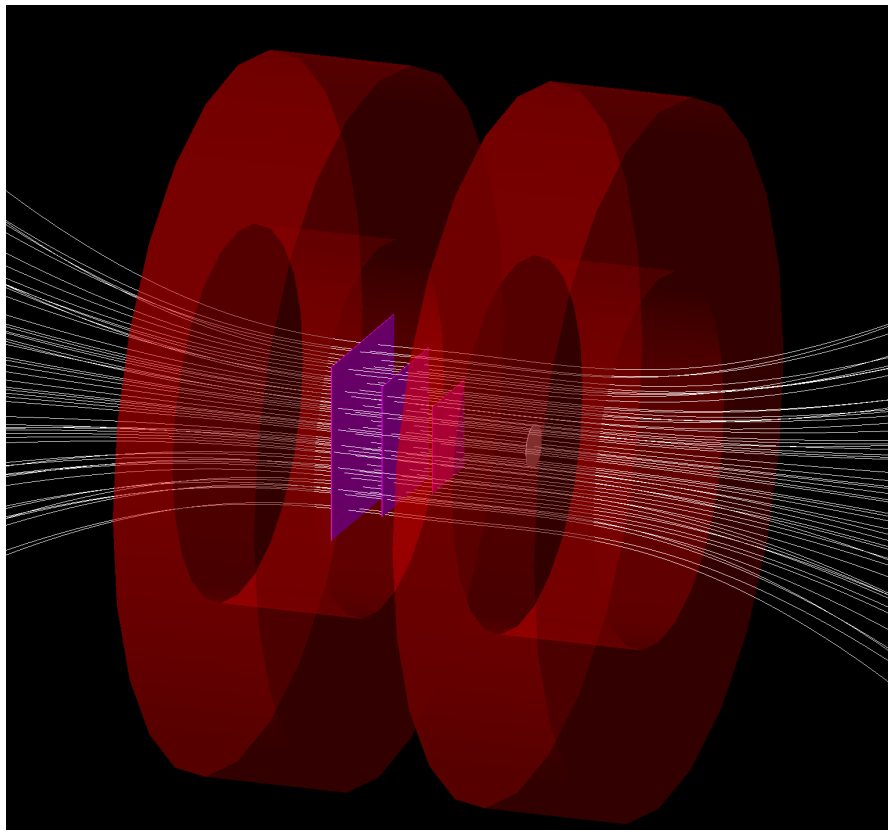
If we do a similar simulation as before but with the up-down setup, we find that the results are extremely similar (dark red = overlap) indicating that, along the axis of the coils, helmholtz coils can produce approximately uniform magnetic fields to a very high precision:



## LAMPF Spectrometer Helmholtz Simulation:

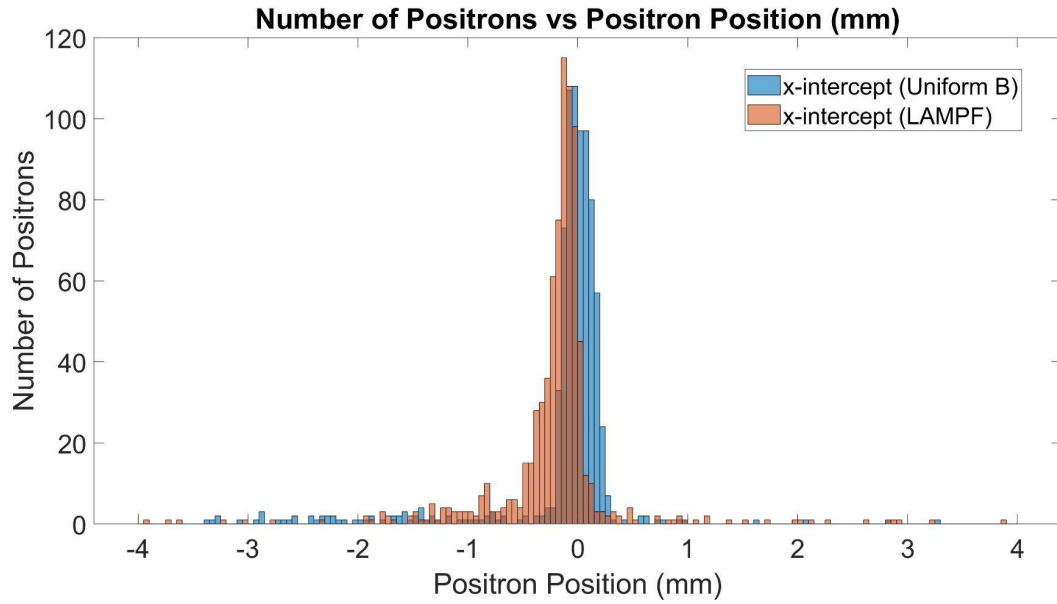
### Front-Back Setup:

If we run a simulation using a helmholtz coil (based on the LAMPF spectrometer in TRIUMF) as shown below:



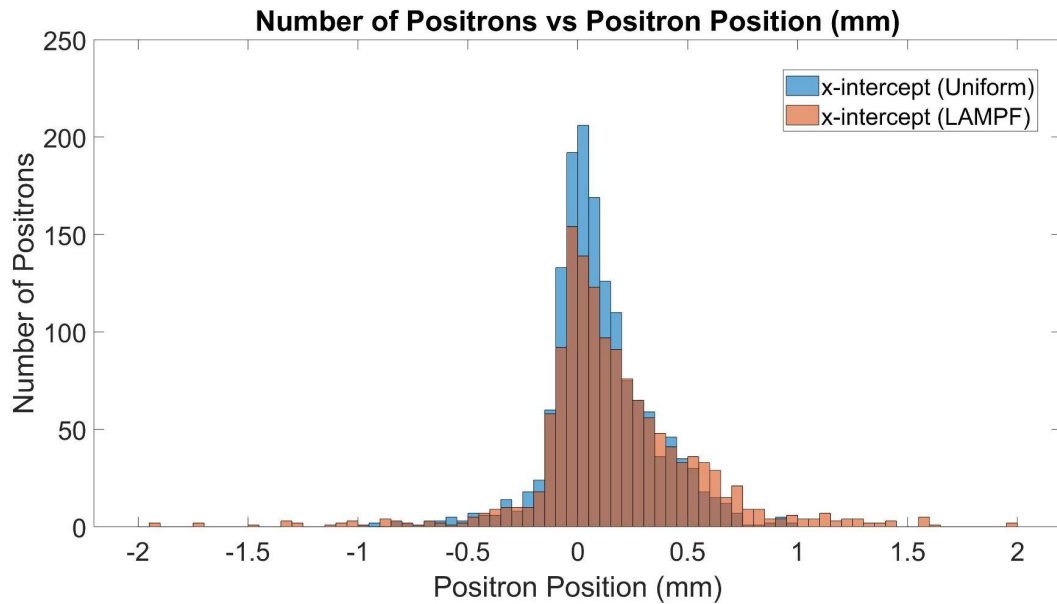
We run into a problem. Specifically, the full simulation takes about 25,000 s (just under 7 hours) assuming the maxStep parameter is kept at 1 mm. We can reduce the simulation time by about a factor of 9 if we change the maxStep parameter to 100 mm. Although the G4Beamline user guide says that changing the maxStep size does not make a significant change in the tracking, I found that the number of positrons detected by the detectors as well as the distribution of the positrons that were detected changed depending on maxStep size (483 detections for maxStep = 1 mm, 498 detections for maxStep = 100 mm).

However, there is a fix to this problem. If we decrease the current from 13,346 Amp to 6 Amp, we find that the simulation runs 100x faster than before. The results of such a simulation are shown below:



### Up-Down Setup:

If we run a simulation with an Up-Down set-up we find that using a LAMPF spectrometer as part of our simulation is slightly less accurate than the exact same simulation but with a uniform magnetic field.



## Conclusion:

All of the simulations above are for future sets of experiments after the summer of 2022 (Experiment number M2246). They are meant to give insight into the design of the setups behind the positron detectors, in order to achieve maximum efficiency and accuracy. We also examine different positron tracking algorithms to determine the origin of the positron.

## Appendix 1: Conference Poster

[MuSR Conference Paper](#)